Nucleosynthesis across the Galaxy: AGB Stars and Neutron Stars Mergers

Diego Vescovi[1,2,3], Sergio Cristallo[2,3], and Marica Branchesi[1,4]

1. Gran Sasso Science Institute (GSSI), L'Aquila, Italy
2. INFN – Section of Perugia, Perugia, Italy
3. INAF – Osservatorio Astronomico d'Abruzzo, Teramo, Italy
4. INFN – Laboratori Nazionali del Gran Sasso, Assergi, Italy

INFN Istituto Nazionale di Fisica Nucleare

GSSI GRAN SASSO SCIENCE INSTITUTE SCHOOL OF ADVANCED STUDIES Scuola Universitaria Superiore

INAF ISTITUTO NAZIONALE DI ASTROFISICA

GSSI Admission to the 3rd year

GSSI - L'Aquila - Italy, 10 October 2019

The origin of heavy elements in the Solar System

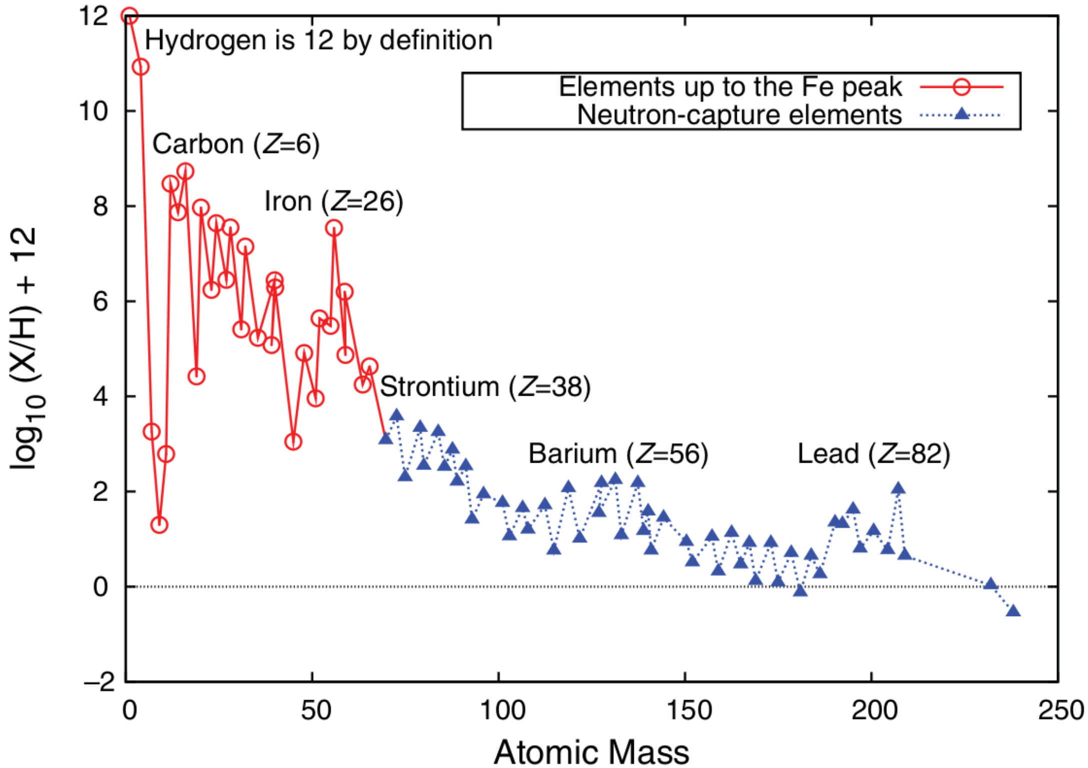

Location of peaks indicates *n*-captures along valley of stability ➡ *s*-process

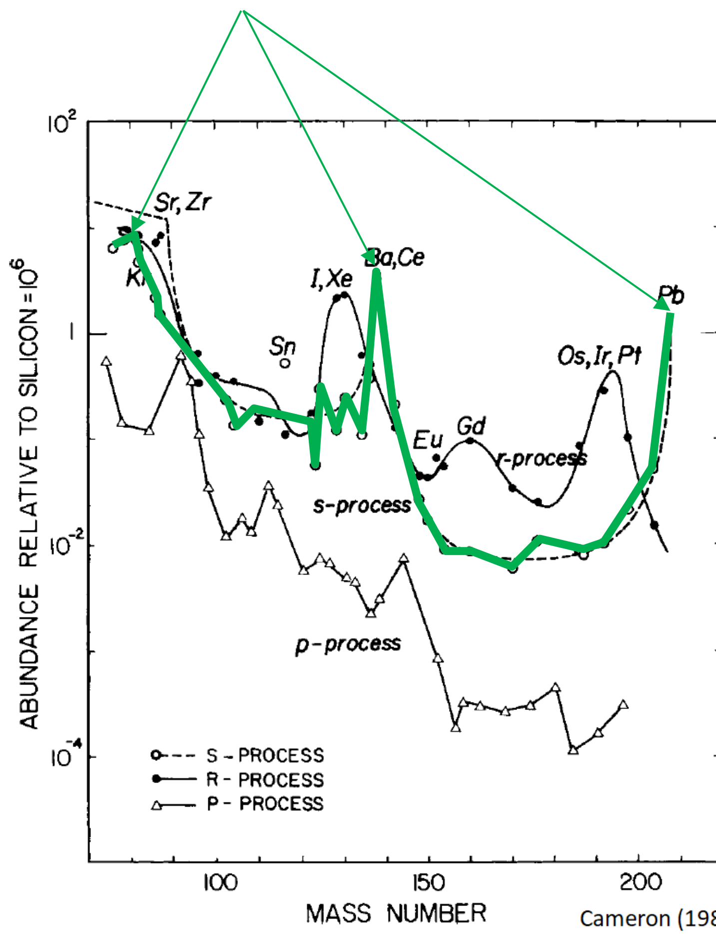

Cameron (1982)

Neutron captures processes :

- *r*-process
- *s*-process
  1) Weak component (A<90)
     Massive Stars
  2) Main component (from Sr to Bi)
     AGB stars

H- and He-burning in TP-AGB stars

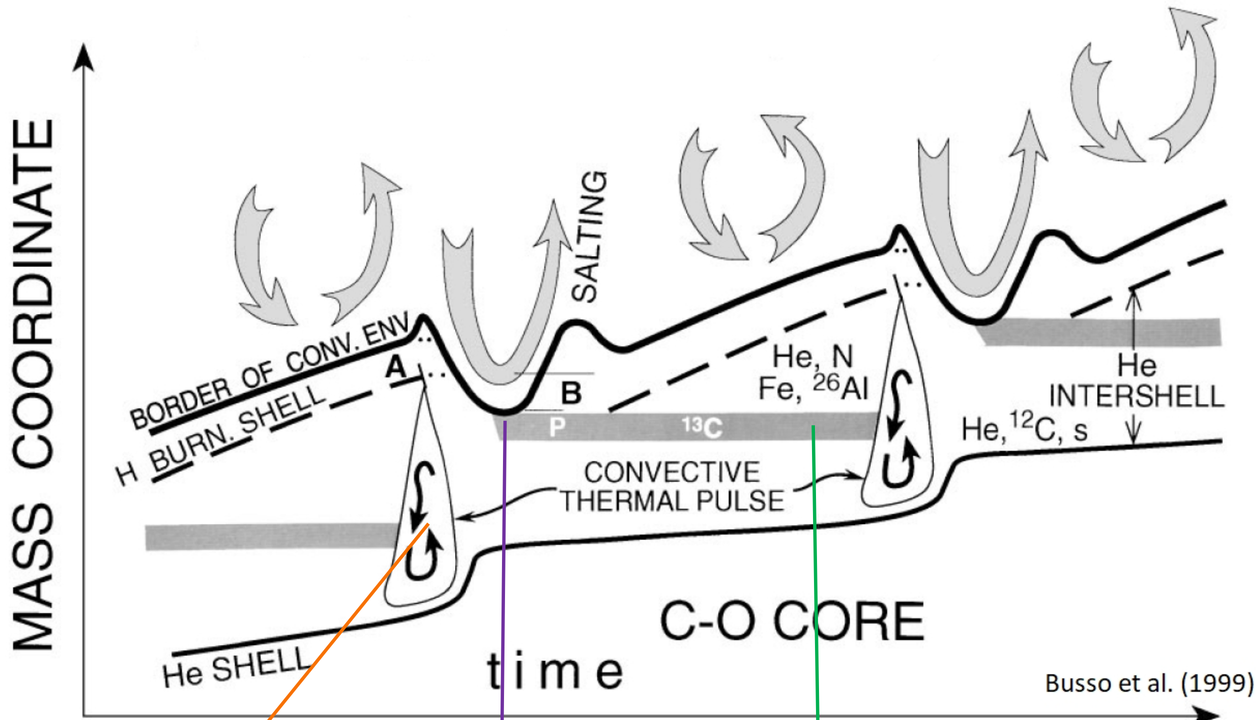

- What?
  Low-Mass Stars
- When?
  Asymptotic Giant Branch (AGB)
- How?
  Thermally Pulsing (TP)

He-flash

proton penetration

^{13}C-pocket

$^{12}C(p,\gamma)^{13}N(\beta^{+}\nu)^{13}C$

$^{22}Ne(\alpha,n)$ —— $^{13}C(\alpha,n)$ ——→ heavy elements!!

The ^{13}C-pocket: formation

- **Protons can penetrate** into the He-rich region at each **TDU (Third Dredge-Up) phenomenon**

Which is the physical mechanism?

Classic models **assume** the ^{13}C-pocket formation

Many recent physical approaches:

- Opacity induced overshoot (Cristallo+ 2009, 2011, 2015)
- Convective Boundary Mixing (Battino+ 2016)
- Magnetic fields (Trippella+ 2016; Palmerini+ 2018)
  ➡ bottom-up mechanism through **magnetic buoyancy**

1a) Rotational shears promote magnetic fields?
1b) Fossil magnetic fields?
2) Magnetic structures reach the envelope
3) Protons are injested into the He-rich region

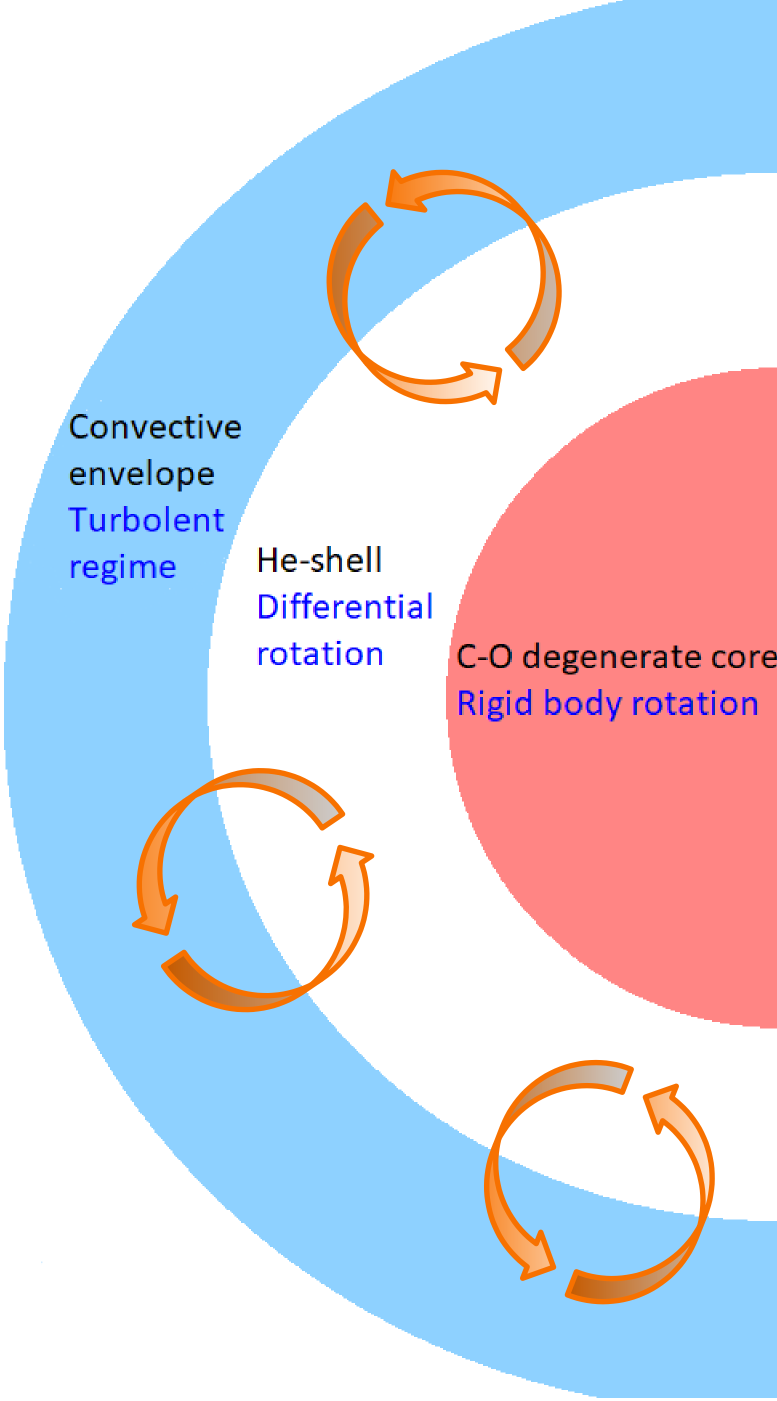

Magnetic buoyancy

- MagnetoHydroDynamics (**MHD**) solutions (Nucci & Busso 2014):
  - ➔ No numerical approximations (exact analytic solution)
  - ➔ Simple geometry: toroidal magnetic field

Equations:

$$\frac{\partial \rho}{\partial t} + \nabla \cdot (\rho \mathbf{v}) = 0$$

$$\frac{\partial \mathbf{B}}{\partial t} - \nabla \times (\mathbf{v} \times \mathbf{B}) - \nu_m \Delta \mathbf{B} = 0$$

$$\rho \left[\frac{\partial \mathbf{v}}{\partial t} + (\mathbf{v} \cdot \nabla)\mathbf{v} - c_d \mathbf{v} + \nabla \Psi \right] - \mu \Delta \mathbf{v} + \nabla P + \frac{1}{4\pi} \mathbf{B} \times (\nabla \times \mathbf{B}) = 0$$

$$\rho \left[\frac{\partial \epsilon}{\partial t} + (\mathbf{v} \cdot \nabla)\epsilon \right] + P \nabla \cdot \mathbf{v} - \nabla \cdot (\kappa \nabla T) + \frac{\nu_m}{4\pi} (\nabla \times \mathbf{B})^2 = 0$$

Solutions:

$$v_r = v_p \left(\frac{r_p}{r} \right)^{k+1}$$

$$B_\varphi = B_{\varphi,p} \left(\frac{r}{r_p} \right)^{k+1}$$

where k is the exponent of the density distribution: $$\rho(r) = \frac{\rho_p}{r_p^k} r^k$$

Implementation

- **Exponential decay** of the convective velocity (Straniero+ 2006, Cristallo+ 2009): ➡ $v = v_{\rm IN} \exp\left(-\frac{\Delta r}{\beta H_p}\right)$

  Parameters:
  - Radius extention of the overshooting region
  - β

- **Magnetic** contribution (**<u>this work</u>**), acting when the density distribution is $\rho \propto r^k$:

$$v_{down}(r) = v(r_p)\frac{\rho(r_p)}{\rho(r_{h+1})}\left(\frac{r_h}{r_p}\right)^{k+2}\left(\frac{r_h}{r}\right)^{k+1}$$

  Parameters:
  - Layer "*p*" at the deepest coordinate from which buoyancy starts (can be identified from the corresponding **critical toroidal B_φ** value) ➡ $B_\varphi \gtrsim \left(4\pi\rho r N^2 H_{\rm p}\frac{\eta}{K}\right)^{1/2}$
  - Starting velocity v_p of the buoyant material

<u>Calibration</u> is needed!

SiC Grains

- Stellar models with **different initial mass** and **metallicity**
  - → different numbers of thermal pulses experienced
  - → different extention of ^{13}C-pockets
- → Isotopic ratios of mainstream grains are <u>quite well reproduced</u>

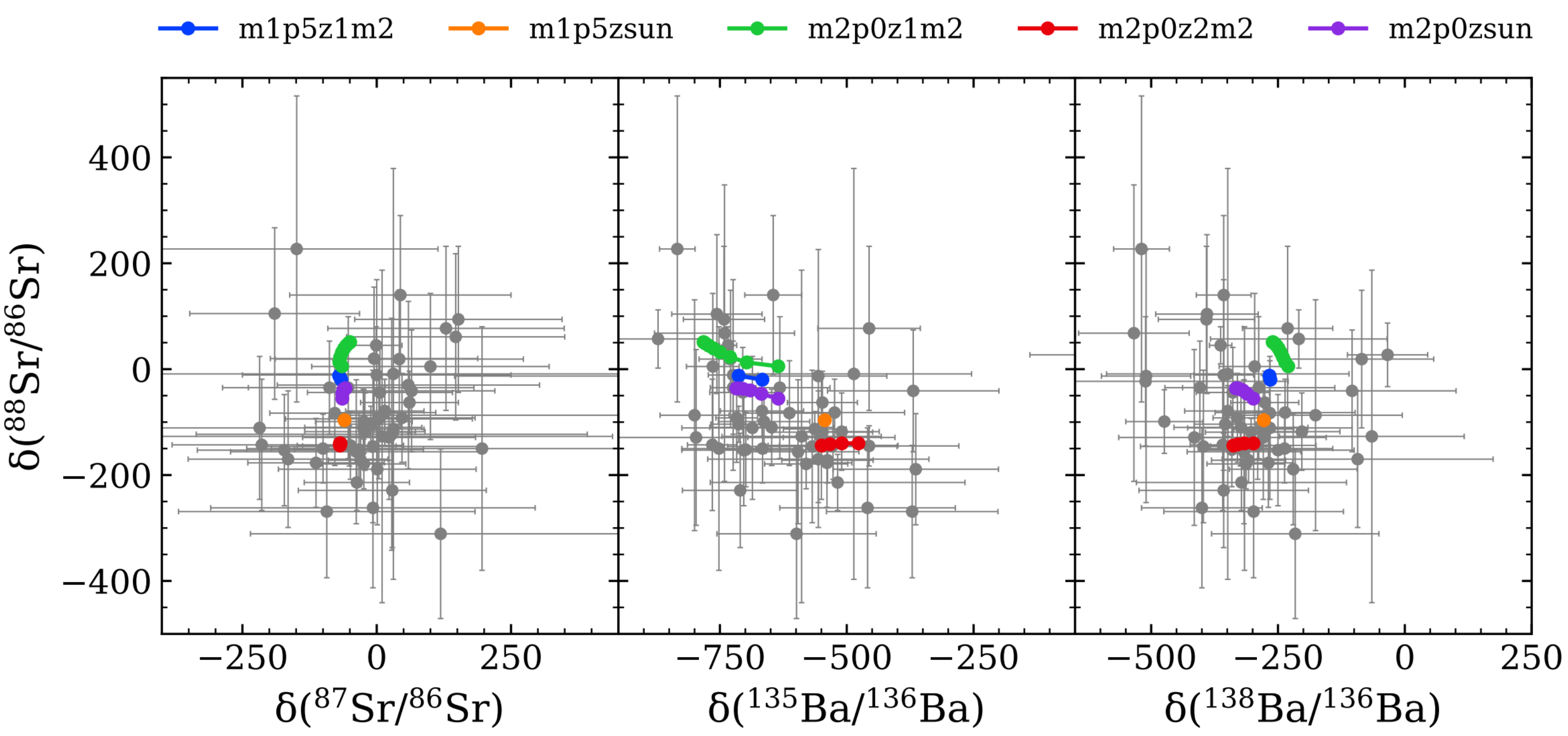

Intrinsic C-rich AGB Stars

- Stellar models with **close-to-solar** metallicity
  - **Low** [hs/ls]
  - **High** [s/Fe]
- Does magnetism <u>fade out</u> for low-to-intermediate mass (3 to 6 $M_\odot$)?

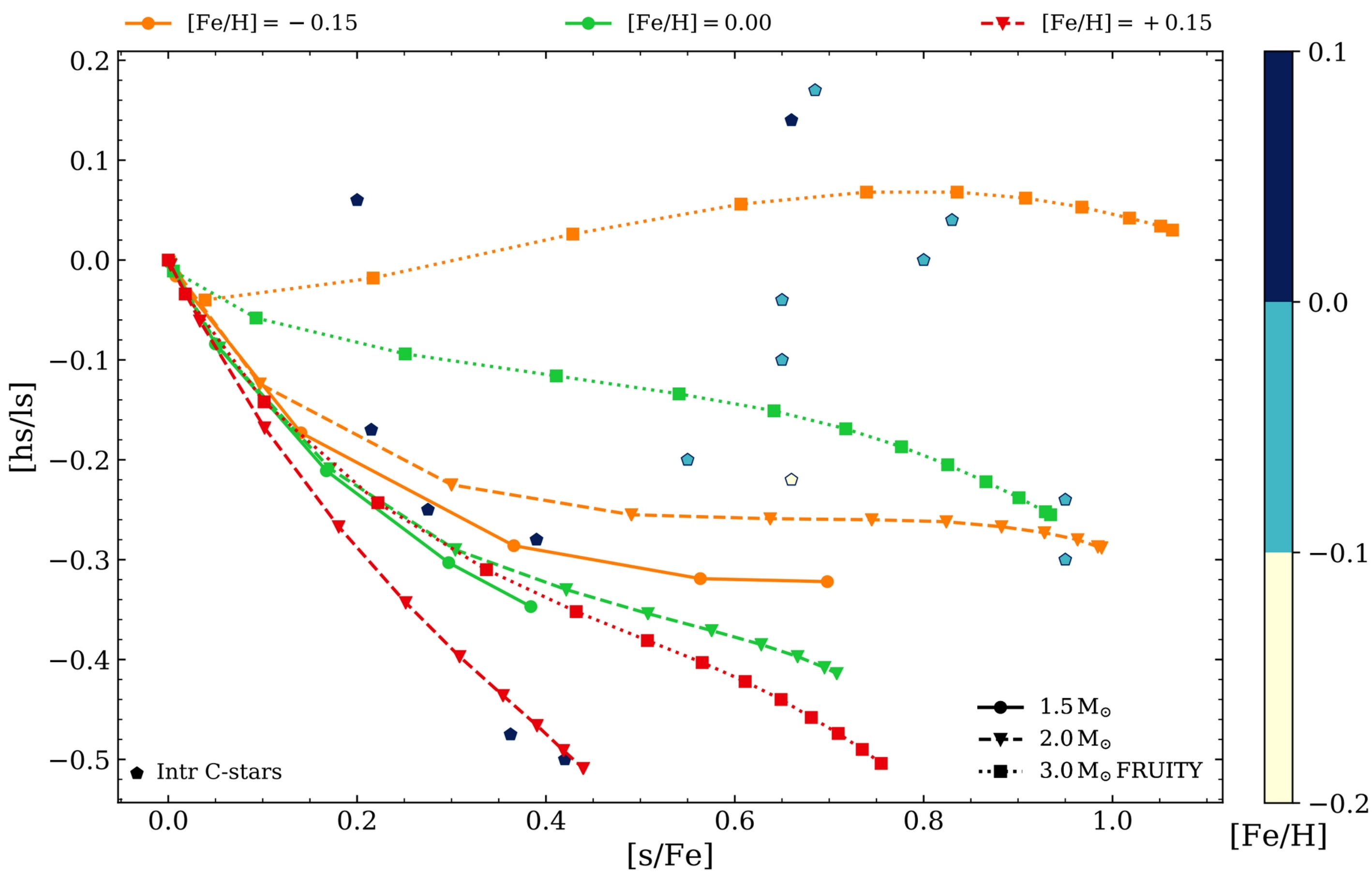

Post- and Intrinsic C-rich AGB Stars I

- Stellar models with **low metallicity**
  - [hs/ls] vs. [s/Fe] **consistent with observations**
  - Models with opacity-induced overshoot only **<u>fail</u>**

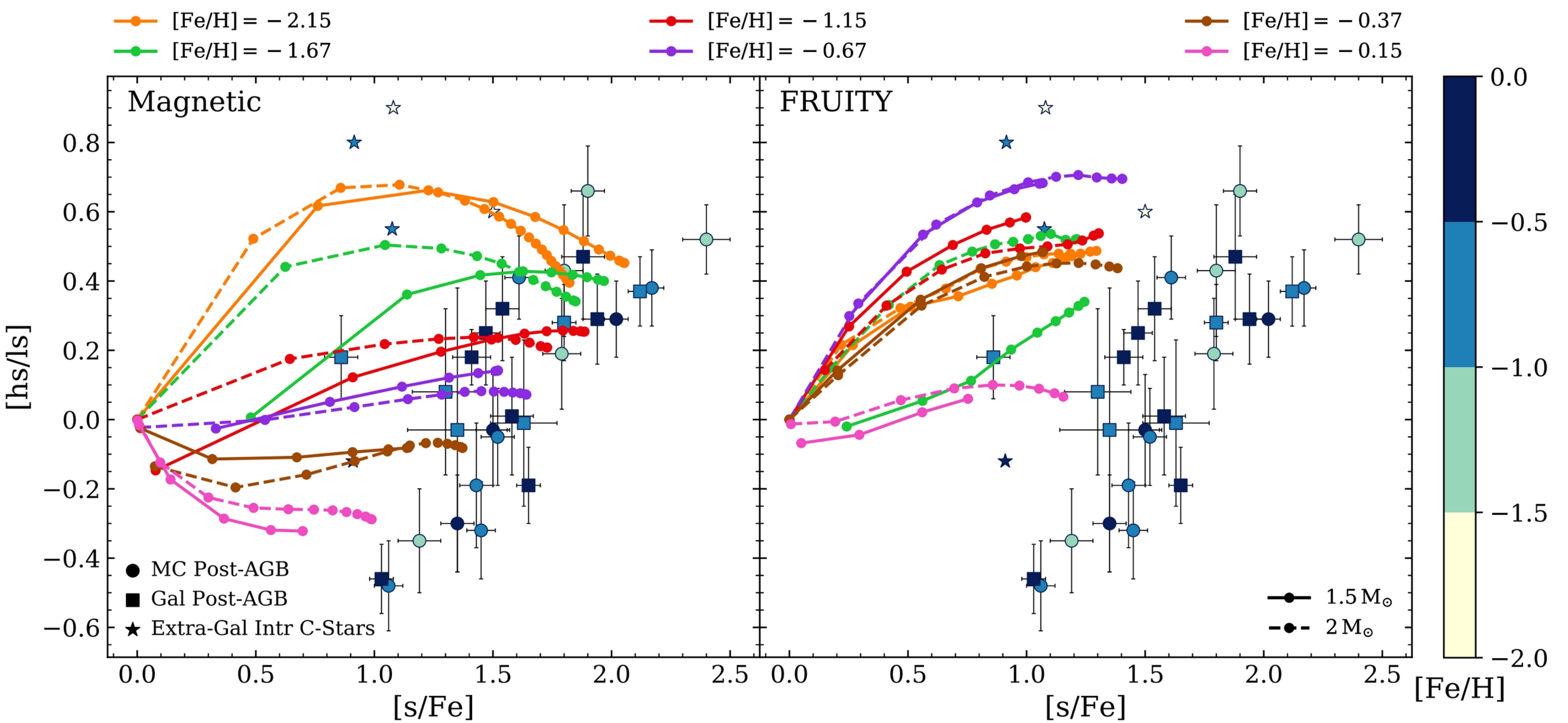

Post- and Intrinsic C-rich AGB Stars II

- Stellar models at different metallicities
  - [hs/ls] vs. [Fe/H] **consistent with observations**
  - Models with opacity-induced overshoot only **fail** again

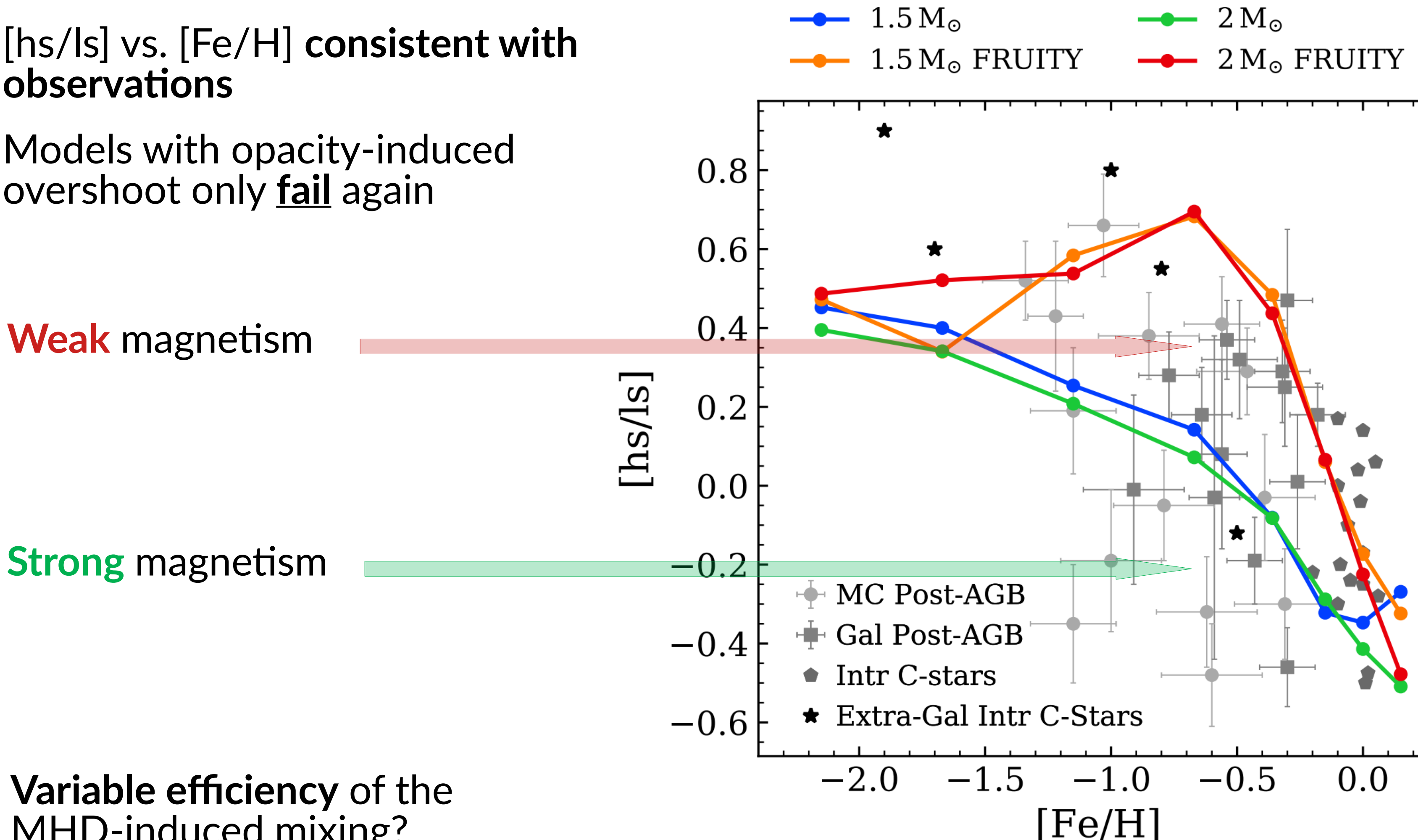

- **Variable efficiency** of the MHD-induced mixing?
- **Mass-dependent efficiency**?

Summary I

- Most of what we know has been learned through a lengthy work with parameterized models, trying to constrain the parameters gradually, from the increasing accuracy of observations
- This allowed recently the development of physical models for the mixing mechanisms required to produce the ^{13}C neutron source.
- Taking into account magnetic fields in radiative regions might be crucial in modeling the mixing episodes (e.g. through **magnetic buoyancy**).
- First outcomes confirms recent results from Trippella+ (2016), Palmerini+ (2018), and Liu+ (2018, 2019)
- **More extended and flatter** ^{13}C-pocket
- The majority of isotopic ratios of mainstream grains are quite well reproduced
- [hs/ls] vs. [s/Fe] and [hs/ls] vs. [Fe/H] **consistent with observations** of post-AGB and intrinsic AGB stars
- Magnetism has (most problably) **variable intensity**

r-process: basic ideas

- key reactions: $(A, Z) + n \leftrightarrow (A + 1, Z) + \gamma$
- *r*-process requires initial high n_n and T
  - high n_n : $\tau_{(n,\gamma)} << \tau_{\beta\text{-}decay}$
  - high n_n and T: $(n, \gamma) \leftrightarrow (\gamma, n)$ along isotopic chain
  - steady abundances intra-chain with one dominant nucleus
- β-decay rates of dominant nuclei regulate inter-chain flow
- equilibrium freeze-out: n_n drops and β-decays take over

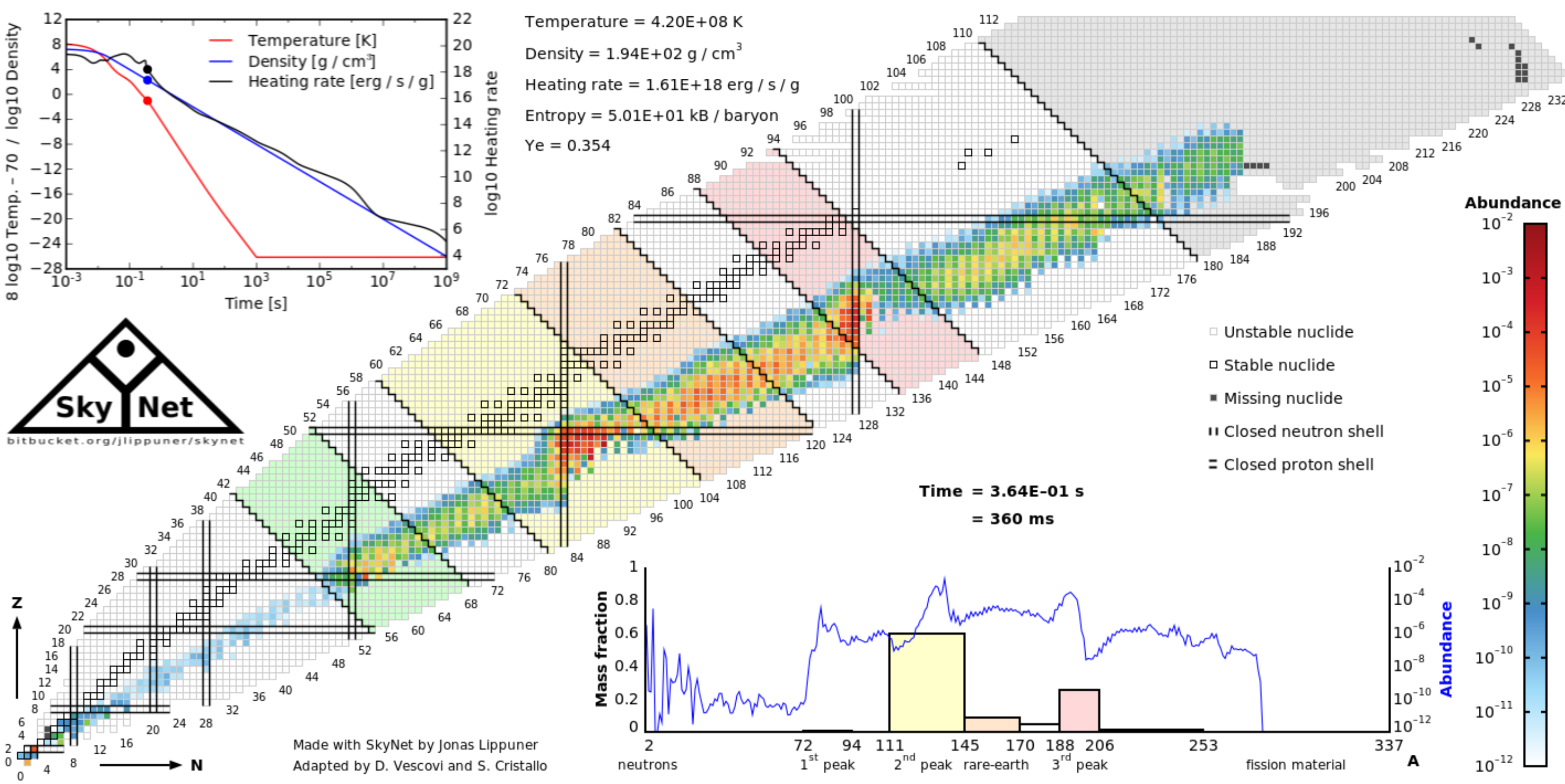

Neutron star mergers as *r*-process site

- *r*-process requires free *n* and seed nuclei (<*A*>, <Z>)
- seed properties/abundances depend on nuclear-statistical equilibrium (NSE) freeze-out
- in adiabatic expansion, neutron-to-seed ratio depends on three parameters:

1) entropy $s \sim T^3/\rho$
2) $Y_e \sim n_p/(n_n+n_p)$
3) τ_{dyn} ($T(t) \approx T_0 \exp(-t/\tau_{dyn})$)

$$n_n/n_{seed} \propto s^3 / (\tau_{dyn} Y_e^3)$$

	high entropy *r*-process	low entropy *r*-process
Possible scenarios	hot CCSN winds	BNS and BHNS mergers MHD supernovae

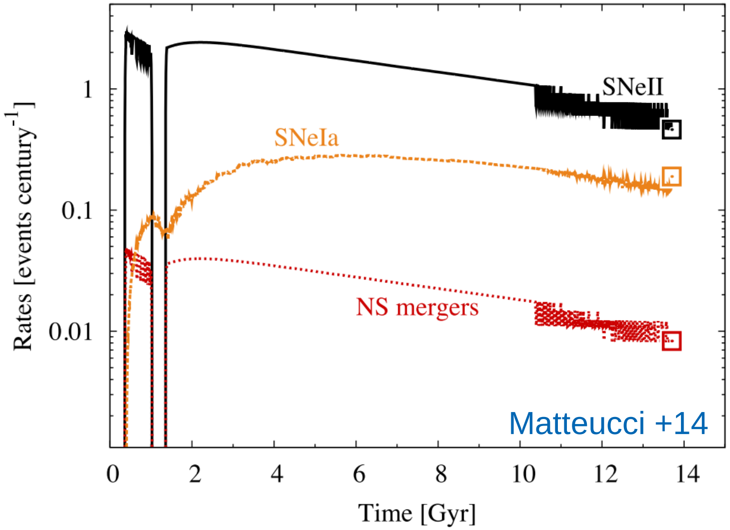

First evidences of *r*-process nucleosynthesis in kilonova from GW170817

BNS merger + kilonova

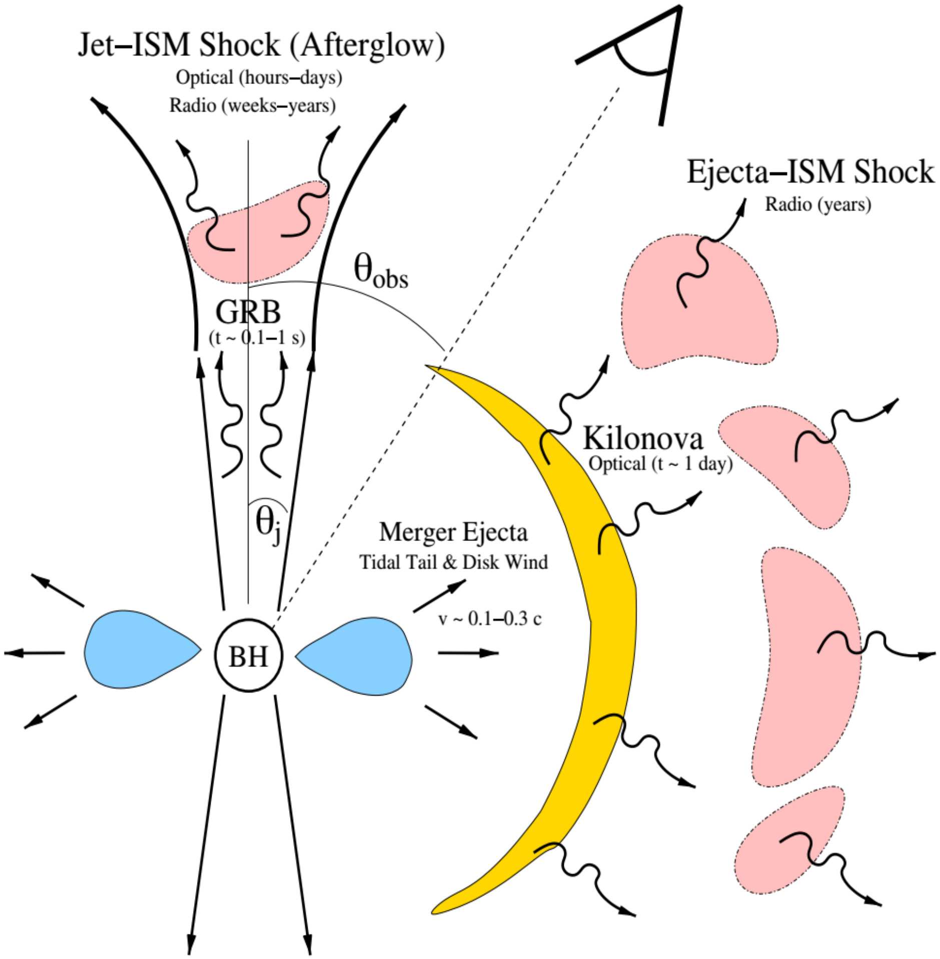

Metzger & Berger 12

Basic ideas:

- radioactive decay of freshly synthetized *r*-process elements in ejecta: release of **nuclear energy**
- thermalization of high energy decay products with ejecta
- **diffusion** of thermal photons during ejecta expansion
- thermal emission of photons at photosphere

Properties of GW170817/AT2017gfo

- 17/08/17, GW+EM detection of an event compatible with BNS merger (LVC PRL 2017)
- rather bright, nIR component, with a peak at ∼ 5 days (red component)
- bright, UV/O component, with a peak at ∼ 1 day (blue component)

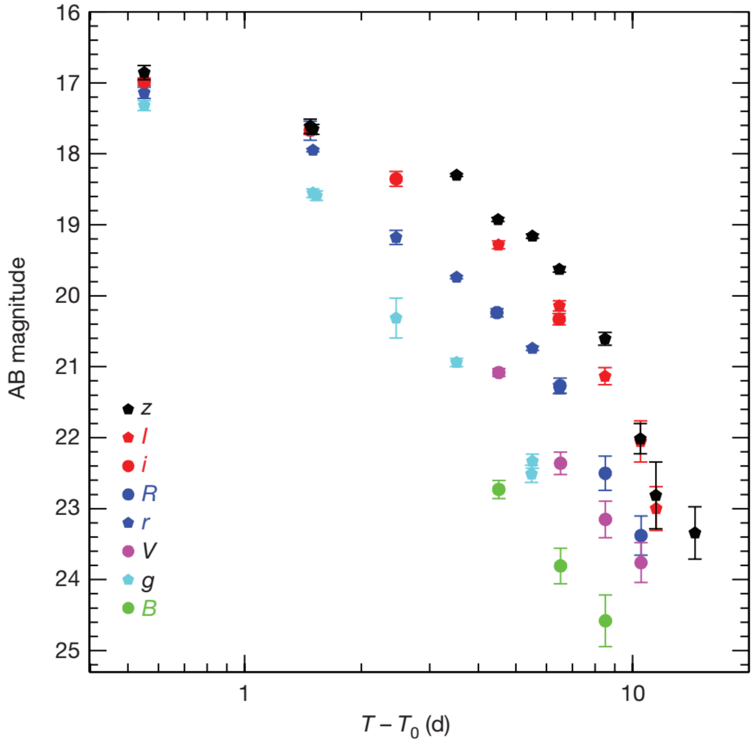

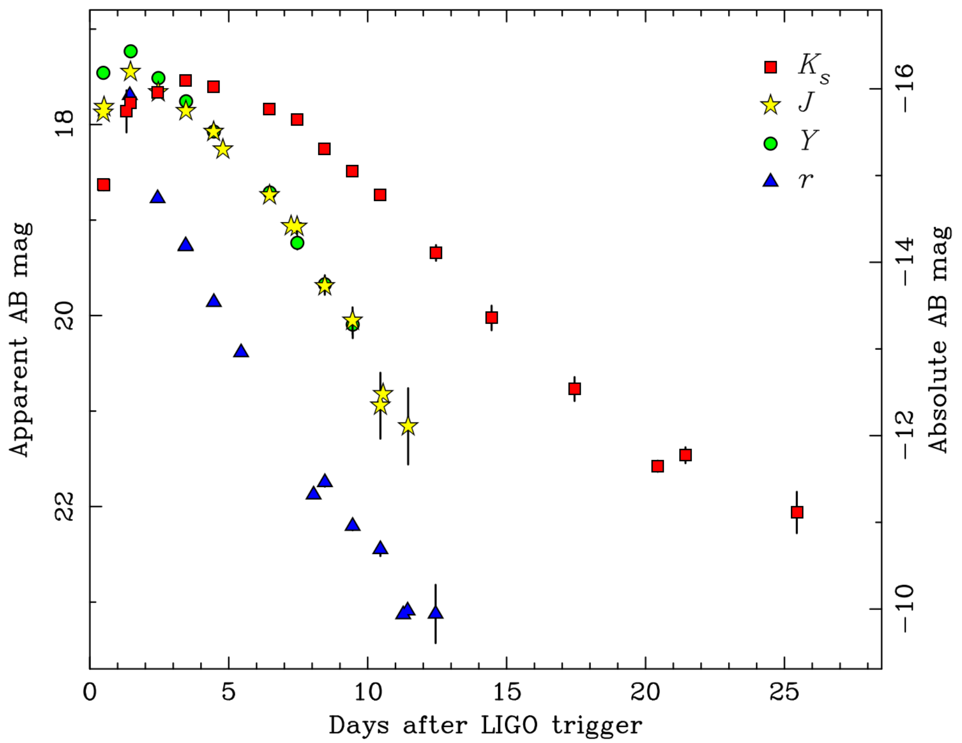

Light curves; Pian, D'Avanzo+ 2017 (left); Tanvir+ 2017 (right)

- Kilonova models fail in explaining the early behavior of the UV and visible light curves
- The presence of a larger nuclear heating rate at t ≲ 1 day **can increase the light curves by half a magnitude during the first day**

Heating rate vs. electron fraction Y_e

- $\dot{Q}$ is usually **approximated** by an analytic fitting formula as $\dot{Q}_{fit}(t) = 10^{10} t_d^{-1.3} erg\, g^{-1} s^{-1}$
- Detailed nucleosynthesis calculations show a complex dependence
- Heating rates normalized to $\dot{Q}_{fit}$ point out that all the **normalized heating rates show considerable excess at different times**

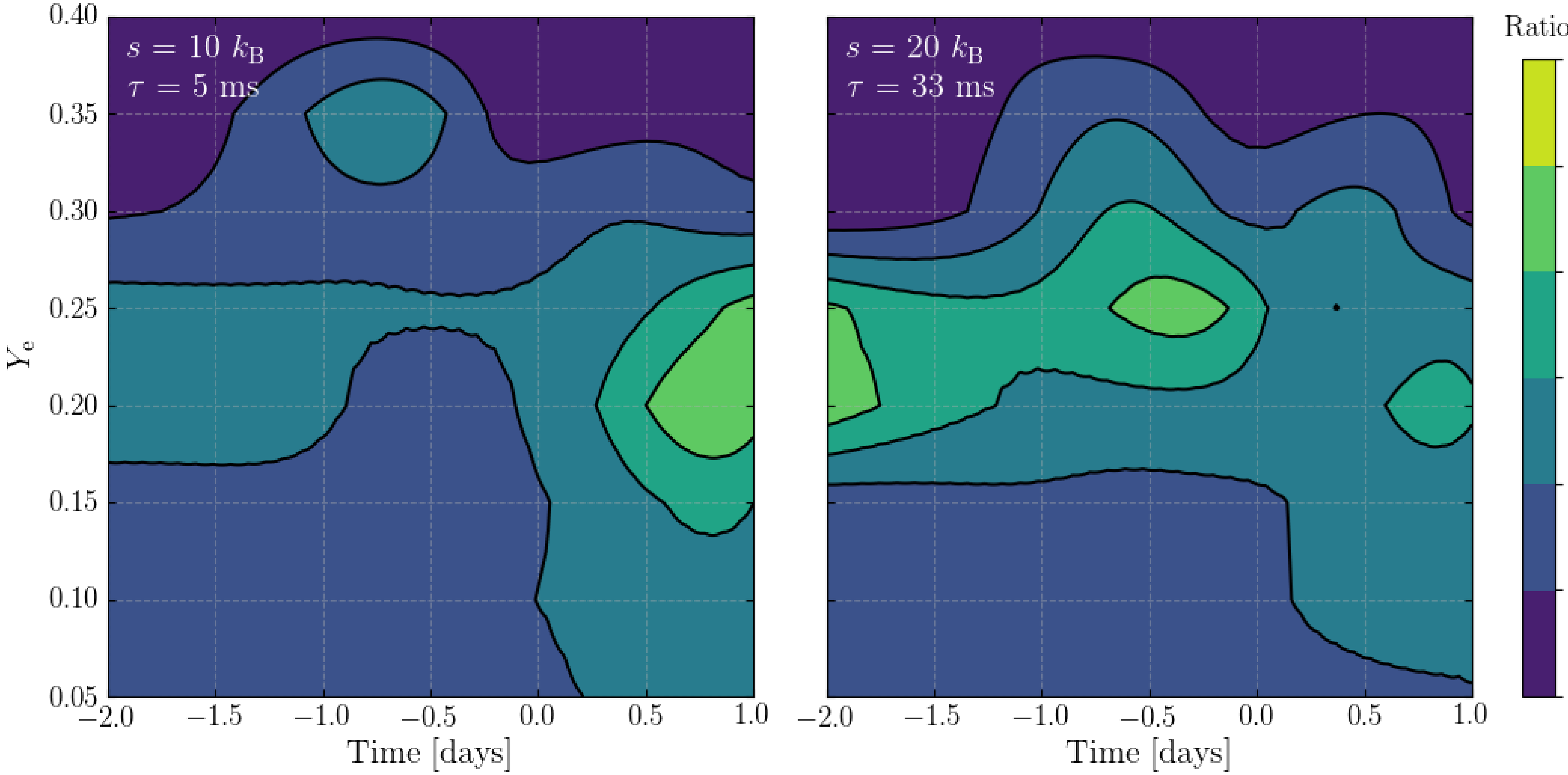

Implementation and first tests

- Inclusion of new detailed nuclear heating rates obtained by nuclear network calculations in an anisotropic, multicomponent kilonova model (Perego+ 2017)
- Coupled with a parallelized Monte Carlo Markov Chain (MCMC) algorithm.
- **Goal:** re-analize AT2017gfo data by computing the posterior distributions associated to several different models

- First outcome (simple isotropic dynamical ejecta) :
  - **brighter lightcurve**

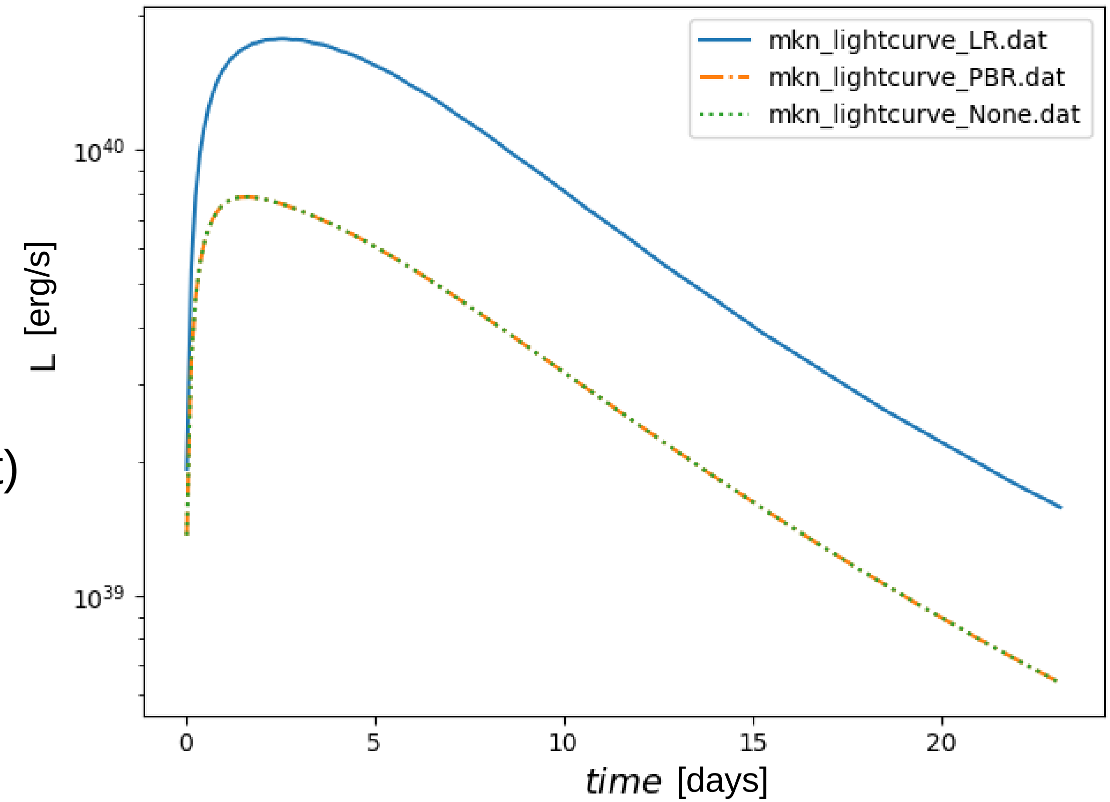

Next steps:

1) different matter ejection mechanisms (multi-component)
2) angular dependence (anisotropy)

Summary II

- Kilonova from GW170817 originates from the **radioactive decay** of heavy elements
- Signature of *r*-process nucleosynthesis in ejecta from neutron star mergers
- Astrophysical site of the *r*-process is identified, but further observations are necessary
- Having identified the astrophysical site it becomes fundamental to **reduce the nuclear physics uncertainties**
- Lanthanide-rich for $Y_e \lesssim 0.25$
- Insensitivity of the abundance pattern to the parameters of the merging system because of an extremely Y_e environment, which guarantees the occurrence of several fission cycles before the *r*-process freezes out
- **Nuclear heating rates are**, at the times relevant for the kilonova emission, **uncertain for a factor a few**
- Kilonova emission seems to be **strongly affected** by non-approximated heating rates

Future work

1) Article on *s*-process nucleosynthesis from magnetic AGB stars, computing low-mass stars (1.5-2 $M_\odot$) at different metallicities. Submission by January/February

2) Analyzing the magnetic contribution to the formation of the ^{13}C neutron source in in low-to-intermediate mass (3-6 $M_\odot$) AGB stars

3) Extend the nuclear network of the open-source Skynet code in order to include the latest available fission rates for *r*-process calculations

4) Perform new 2- and 3-component kilonova model of AT2017gfo, also considering an angular dependence due to anisoptropy of ejecta. Expected draft in the next few months

5) ?? Implement a simplified gray radiative transport scheme (instead of a revised Arnett's model) in order to compute the lightcurve

Backup Slides

SiC Grains II

- We considered **isotopic data** including Sr and Ba isotope ratios in **presolar SiC grains**.
- We considered **magnetic contribution** to the partial mixing of hydrogen.
- **One stellar model**: $2M_{\odot}$ $Z=Z_{\odot}$
- **Fixed** value of β (0.1) and maximum envelope penetration (1.7 H_p)
- **Variable** v_p (2, 4, 6 x10^{-5} cm s^{-1}) and B_{φ} (0.5, 1, 2 x10^{5} G)

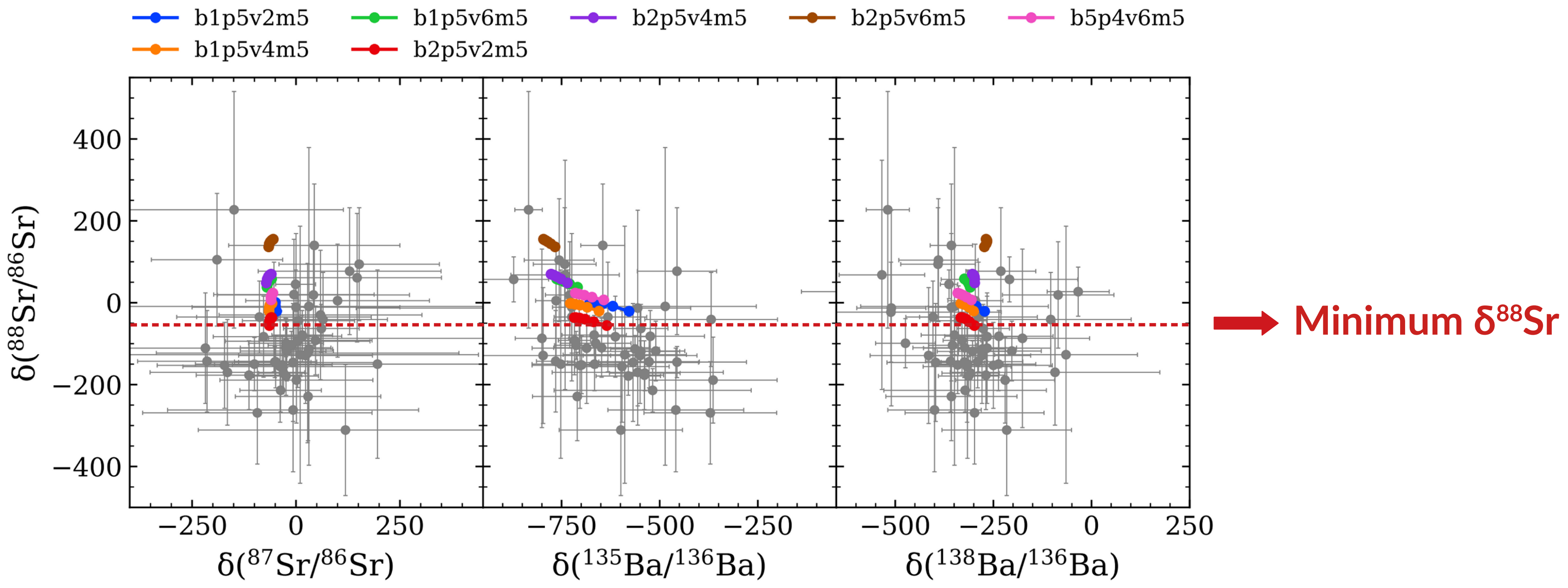

The ^{13}C-pocket: parametric space

- Our **current** best (not yet definitive) choice can be summarized as:

Parameter	Adopted value	References or motivation
v_p	2×10^{-5} cm/s	Best fit to the grains data
β	0.1	Cristallo+ 2009
Radius extention of the overshooting region	1.7 Hp	Same amount of H-depleted dredged-up material of FRUITY
Layer from which buoyancy starts (critical toroidal B_φ value)	2×10^5 G	Best fit to the grains data

Magnetic field in O-rich and C-rich AGB stars

- Generally, AGB magnetic field measurements come from maser polarization observations (SiO, H2O and OH) (e.g. Vlemmings+ 2012)
- These have revealed a strong magnetic field throughout the circumstellar envelope
- **B-field at surface ~ few G**
- Although the maser observations trace only oxygen-rich AGB stars, recent CN Zeeman splitting observations (Duthu+ 2017) indicate that **similar strength fields are found around C-rich stars**

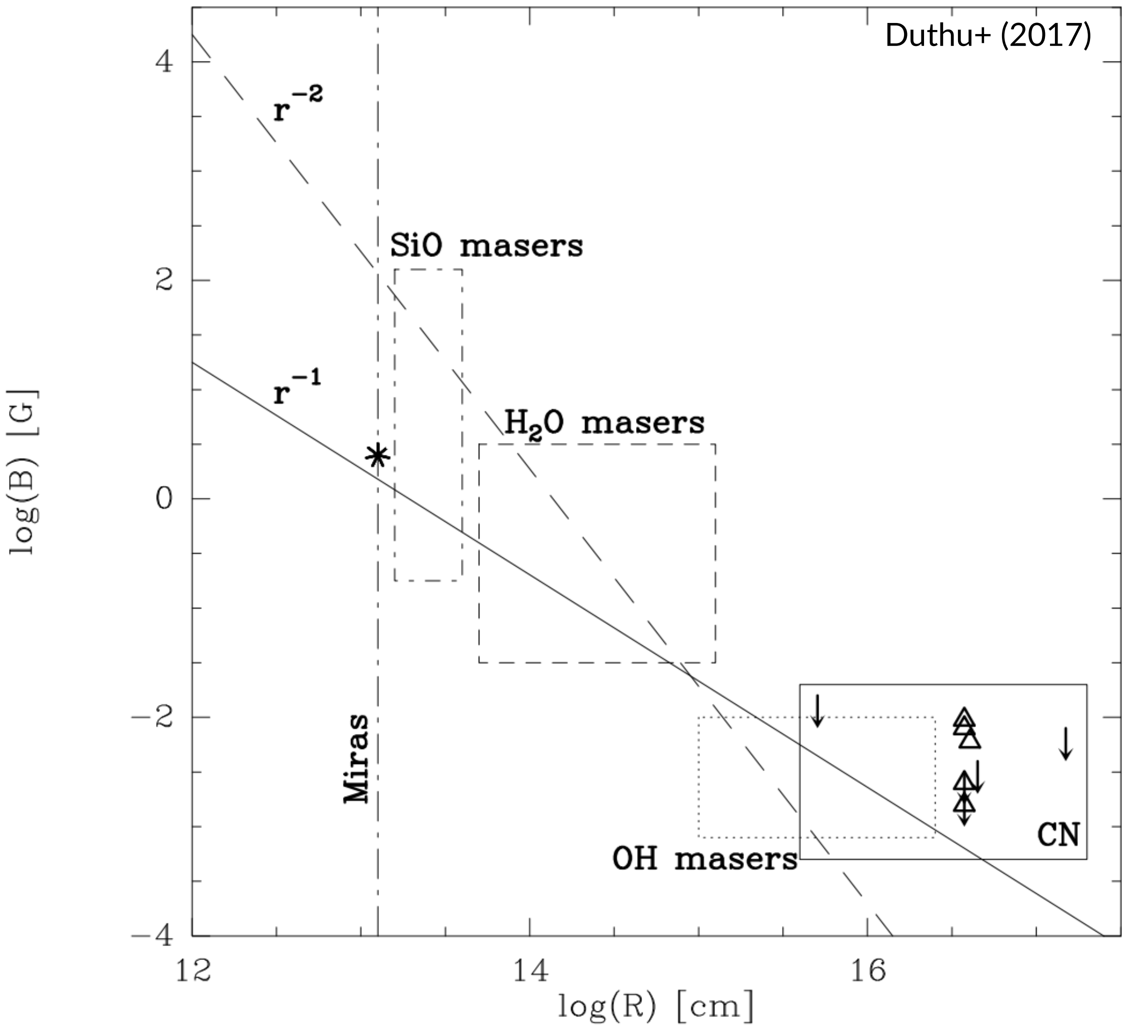

Critical toroidal B-field

- Stellar model: $2M_\odot$ $Z=Z_\odot$

- **The critical B_φ** necessary for the onset of magnetic buoyancy instabilities, in radiative zone below the convective envelope **varies from ~10^4G to ~10^6G**

- Different values of B_φ correspond to different values of the free parameter r_p

→ The strength of **B_φ determines the extension** of the mixed zone and, in turn, **of the 13C-pocket**

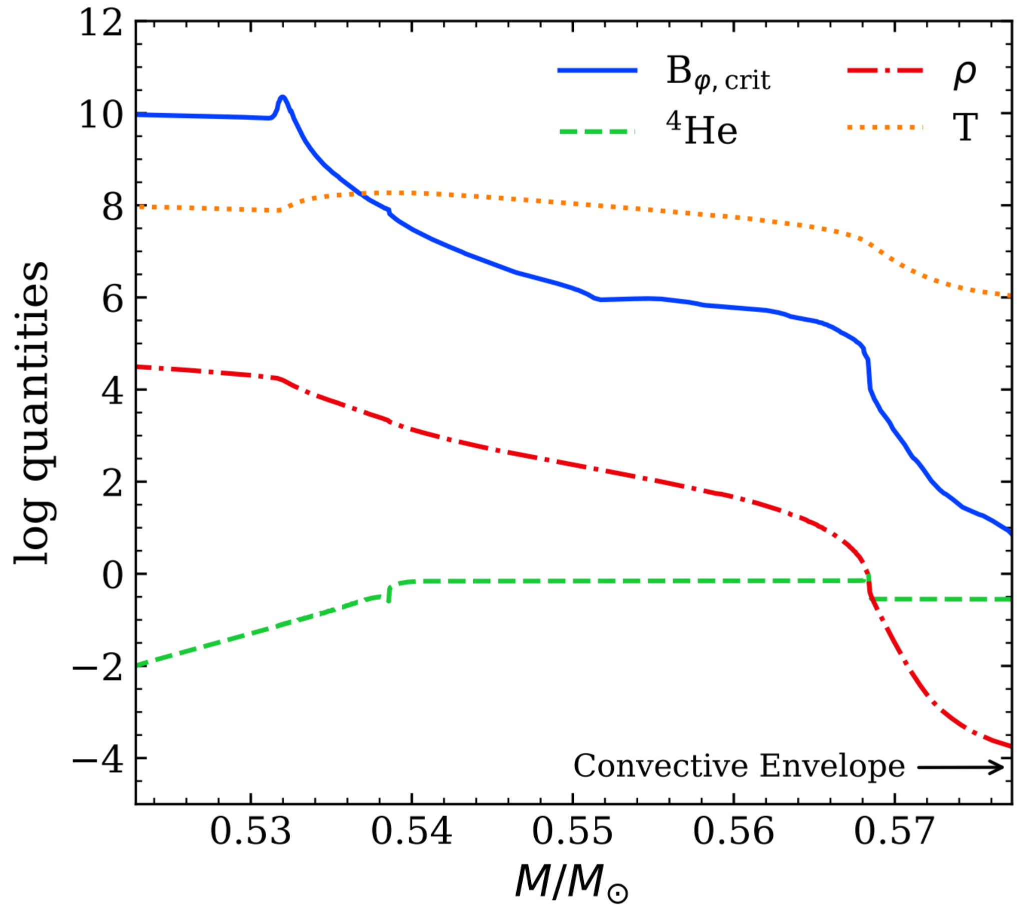

Generation of a toroidal B-field in the He-intershell

- Stellar model: 2.5$M_\odot$ $Z=Z_\odot$
- Stretching of a preexisting **poloidal field** can generate a toroidal field

$$\Rightarrow \frac{\partial B_\varphi}{\partial t} = \frac{1}{r}\frac{\partial}{\partial r}\left(\Omega r^2 B_\mathrm{p}\right) = \Omega q B_\mathrm{p}$$

- Differential rotation in the He-intershell?
- An additional artificial viscosity of around $10^7 \mathrm{cm^2 s^{-1}}$ provides a sufficient transport of angular momentum to match the core and envelope rotation rates for core He-burning stars (den Hartogh + 2019a,b)
- The **critical polidal B_p** would be

$$\Rightarrow B_\mathrm{p} \sim B_\varphi (\Omega q \Delta t)^{-1}$$

- A rough (preliminary) estimate gives a **B_p few hundreds times lower than B_φ** → **$B_p \lesssim$ 1kG** Not implausible!!

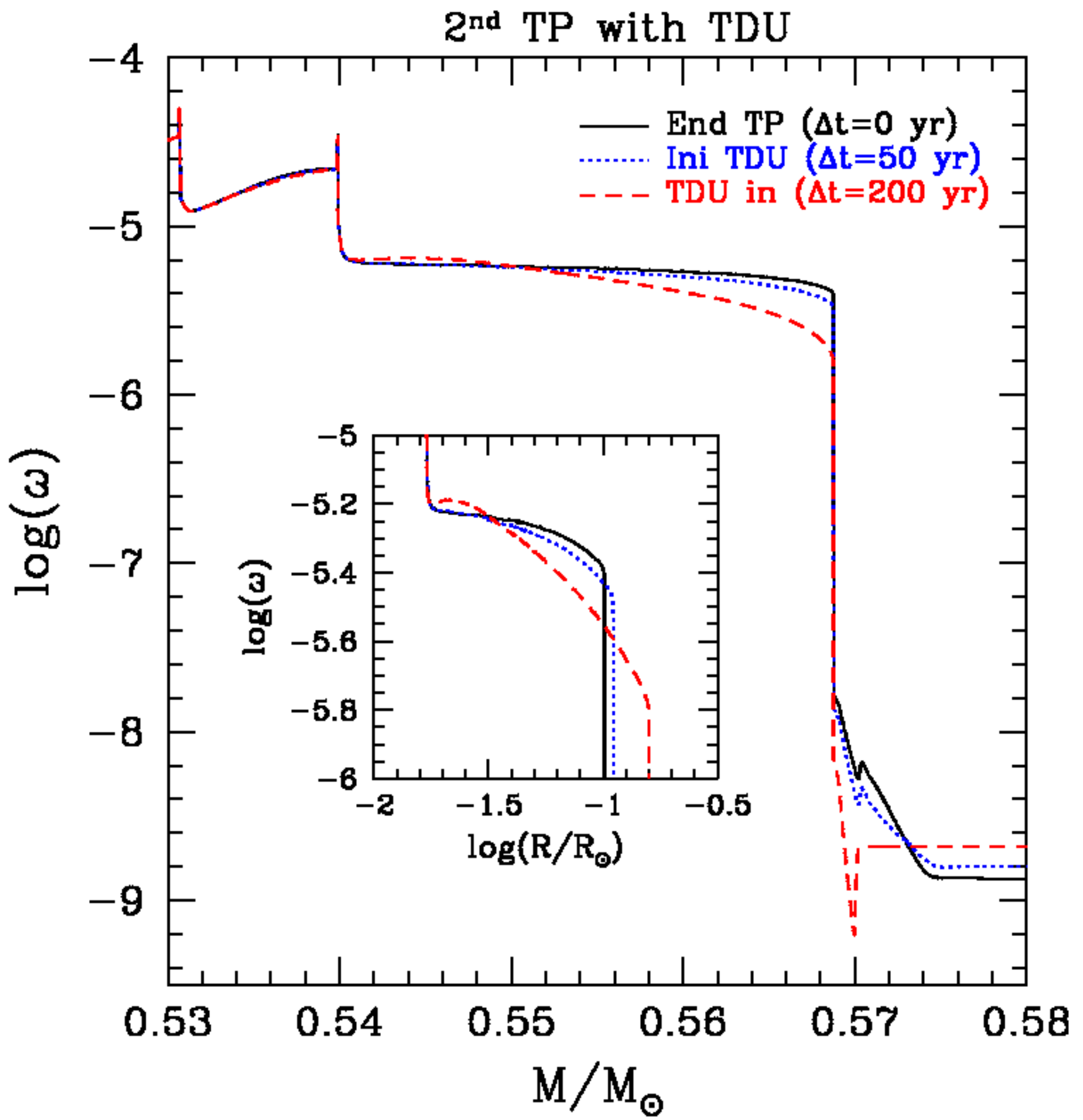

Effective ^{13}C*

- **One stellar model:** $2M_{\odot}$ $Z=Z_{\odot}$
- **Same** sequence TP-interpulse
- **Variable** v_p (2, 4, 6 x10^{-5} cm s^{-1}) and B_{φ} (0.5, 1, 2 x10^5 G)

  → The amount of effective ^{13}C is strongly affected by the adopted parameters

  → The greater the initial velocity of flux tubes and the deeper the buoyancy starts, the **greater the velocity of the downflow material** is

  → Larger values of B_{φ} correspond not only to **larger ^{13}C-pockets** but also to **larger amounts of ^{13}C**

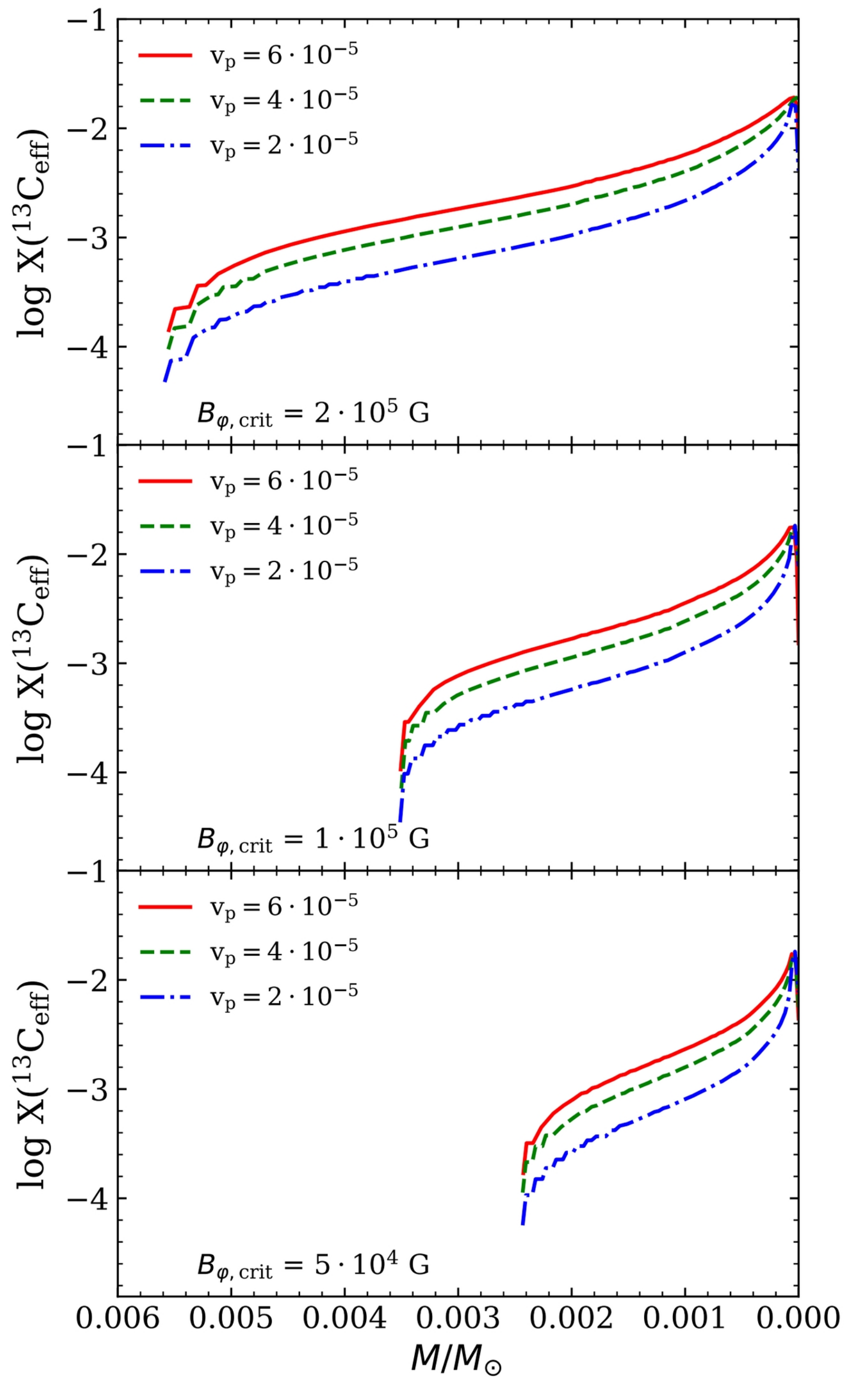

*The mass fraction of effective ^{13}C in a given mesh point is $X(^{13}C_{eff}) = X(^{13}C) - 13/14 * X(^{14}N)$

The ^{13}C-pocket: shape

- Isotopic abundances during the 2nd TDU: ^{1}H, ^{13}C, ^{14}N
- Stellar model: 2$M_{\odot}$ Z=$Z_{\odot}$

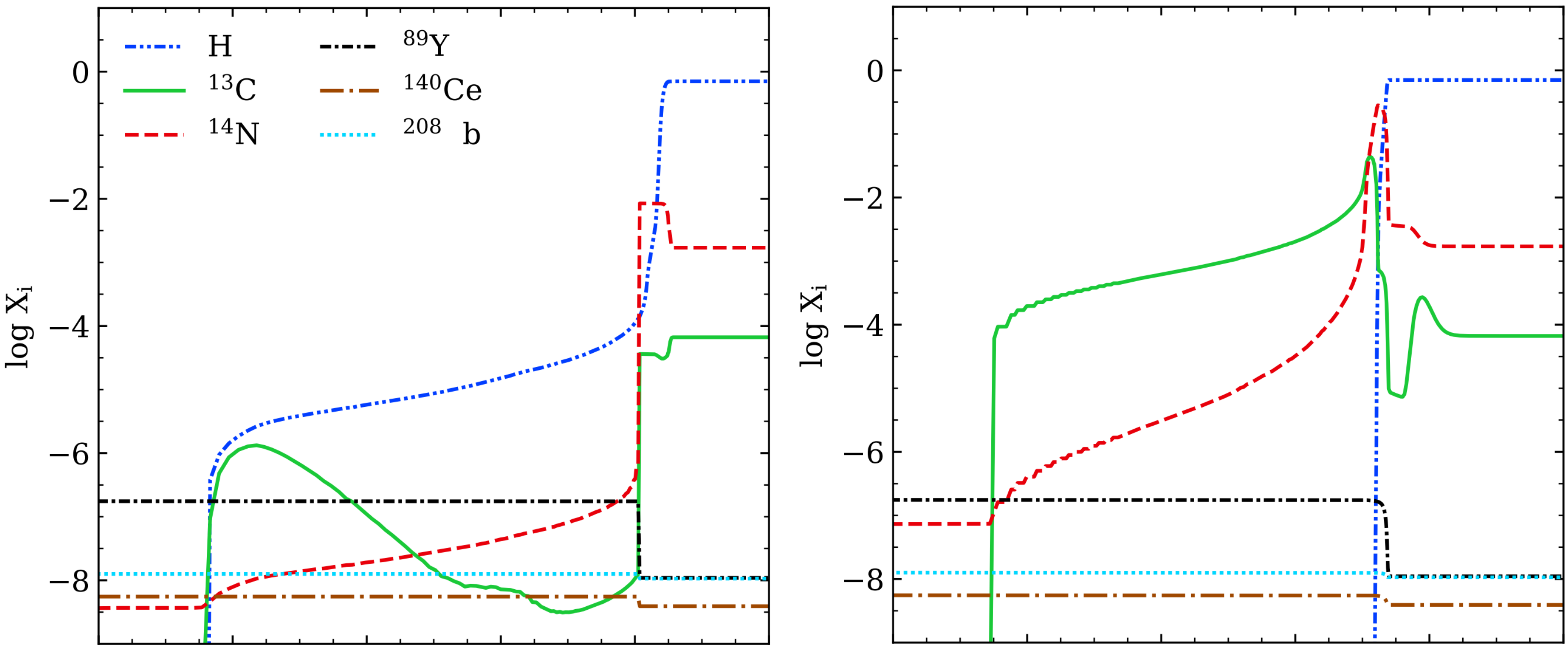

→ An efficient s-process occurs when ^{13}C overcomes ^{14}N

→ Outcome: more extended and a flatter ^{13}C-pocket.

MHD equations

$$\frac{\partial \rho}{\partial t} + \nabla \cdot (\rho \mathbf{v}) = 0 \tag{1}$$

$$\rho \left[\frac{\partial \mathbf{v}}{\partial t} + (\mathbf{v} \cdot \nabla)\mathbf{v} - c_d \mathbf{v} + \nabla \Psi \right] - \mu \Delta \mathbf{v} + \nabla P + \frac{1}{4\pi} \mathbf{B} \times (\nabla \times \mathbf{B}) = 0 \tag{2}$$

$$\frac{\partial \mathbf{B}}{\partial t} - \nabla \times (\mathbf{v} \times \mathbf{B}) - \nu_m \Delta \mathbf{B} = 0 \tag{3}$$

$$\nabla \cdot \mathbf{B} = 0 \tag{4}$$

$$\rho \left[\frac{\partial \epsilon}{\partial t} + (\mathbf{v} \cdot \nabla)\epsilon \right] + P \nabla \cdot \mathbf{v} - \nabla \cdot (\kappa \nabla T) + \frac{\nu_m}{4\pi} (\nabla \times \mathbf{B})^2 = 0.$$

In the above equations, ϵ is the internal energy per unit mass. P, T, and ρ are the pressure, temperature, and density of the plasma, and κ is the thermal conductivity. $\mathbf{B}$ is the magnetic induction field, $\mathbf{v}$ is the plasma velocity, μ is the dynamic viscosity (the product of density and the kinematic viscosity η), and $\mu \Delta \mathbf{v}$ is a simplified form often used for the viscous force per unit volume in stellar MHD (it would formally hold for incompressible fluids with constant μ). Ψ is the gravitational potential, and ν_m is the magnetic diffusivity. The term $c_d \mathbf{v}$ represents the aerodynamic drag force per unit mass.

Magnetic contribution to the downward velocity

$$\rho(r_p)V(r_p) = \rho(r_h)V(r_h)$$

$$4\pi^2 B(r_p)a(r_p)r_p = 4\pi^2 B(r_h)a(r_h)r_h$$

$$\rho_{up,h}v_{up,h} = \rho_{down,h}v_{down,h}$$

$$v_{up,h} = v(r_p)\left(\frac{r_p}{r_h}\right)^{k+1}$$

$$v_{down,h} = v(r_p)\frac{\rho(r_p)}{\rho(r_{h+1})}\frac{a(r_p)}{a(r_h)}$$

$$v_{down}(r) = v_{down,h}\left(\frac{r_h}{r}\right)^{k+1}$$

$$v_{down}(r) = v(r_p)\frac{\rho(r_p)}{\rho(r_{h+1})}\left(\frac{r_h}{r_p}\right)^{k+2}\left(\frac{r_h}{r}\right)^{k+1}$$

➡ The velocity of the downward material is proportional to $v_p r_p^{(-k+2)}$ (with $k \geq -1$)

Final abundances vs. electron fraction Y_e

- **Threshold value $Y_{e,crit} \approx 0.25$**

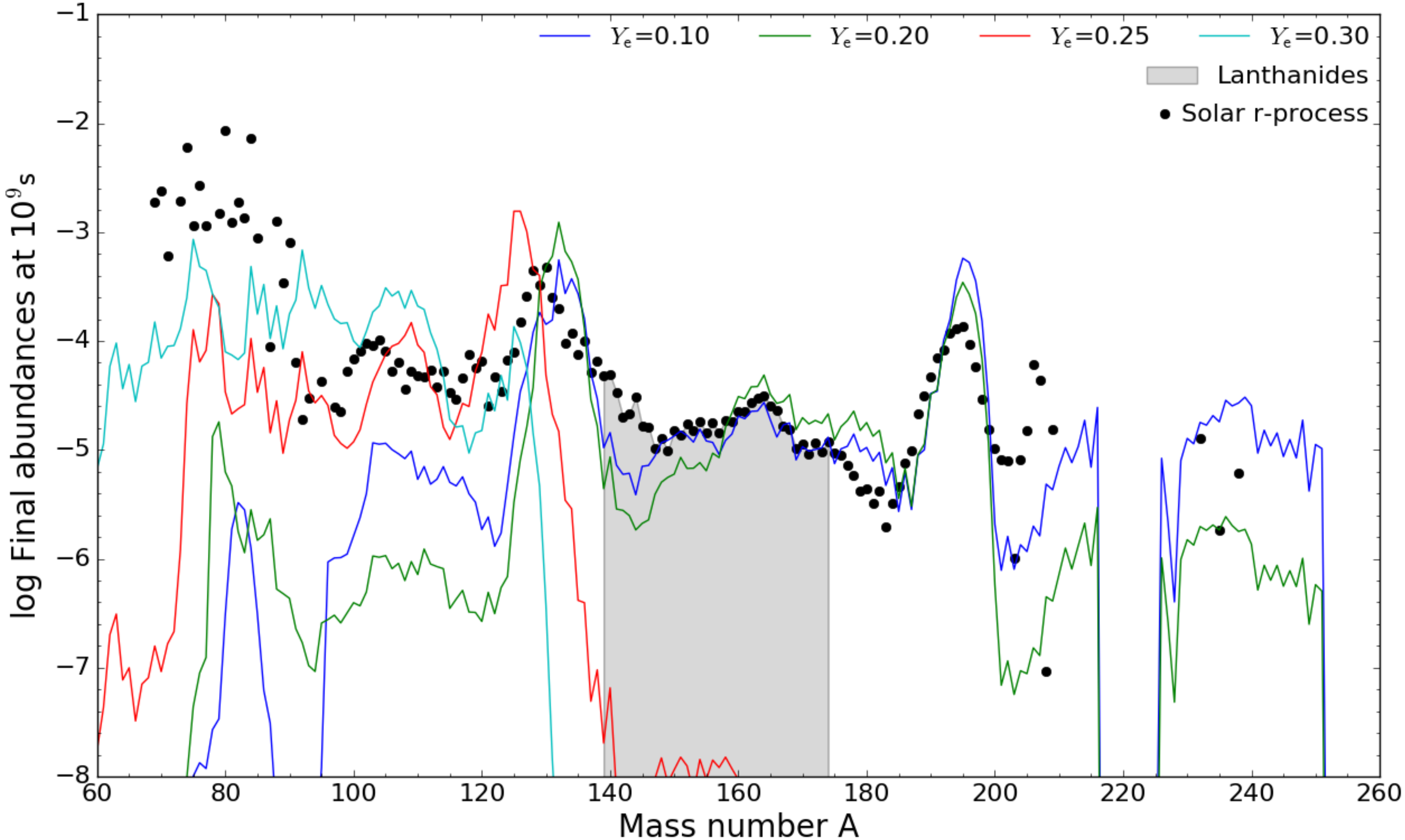

$Y_e < Y_{e,crit}$	$Y_e > Y_{e,cri}$
"robust" *r*-process A ≳ 130	"weak" *r*-process A ≲ 130
insensitive to details of trajectory	sensitive to details of trajectory

Role of fission for the robust r-process

- Simulation starts at NSE

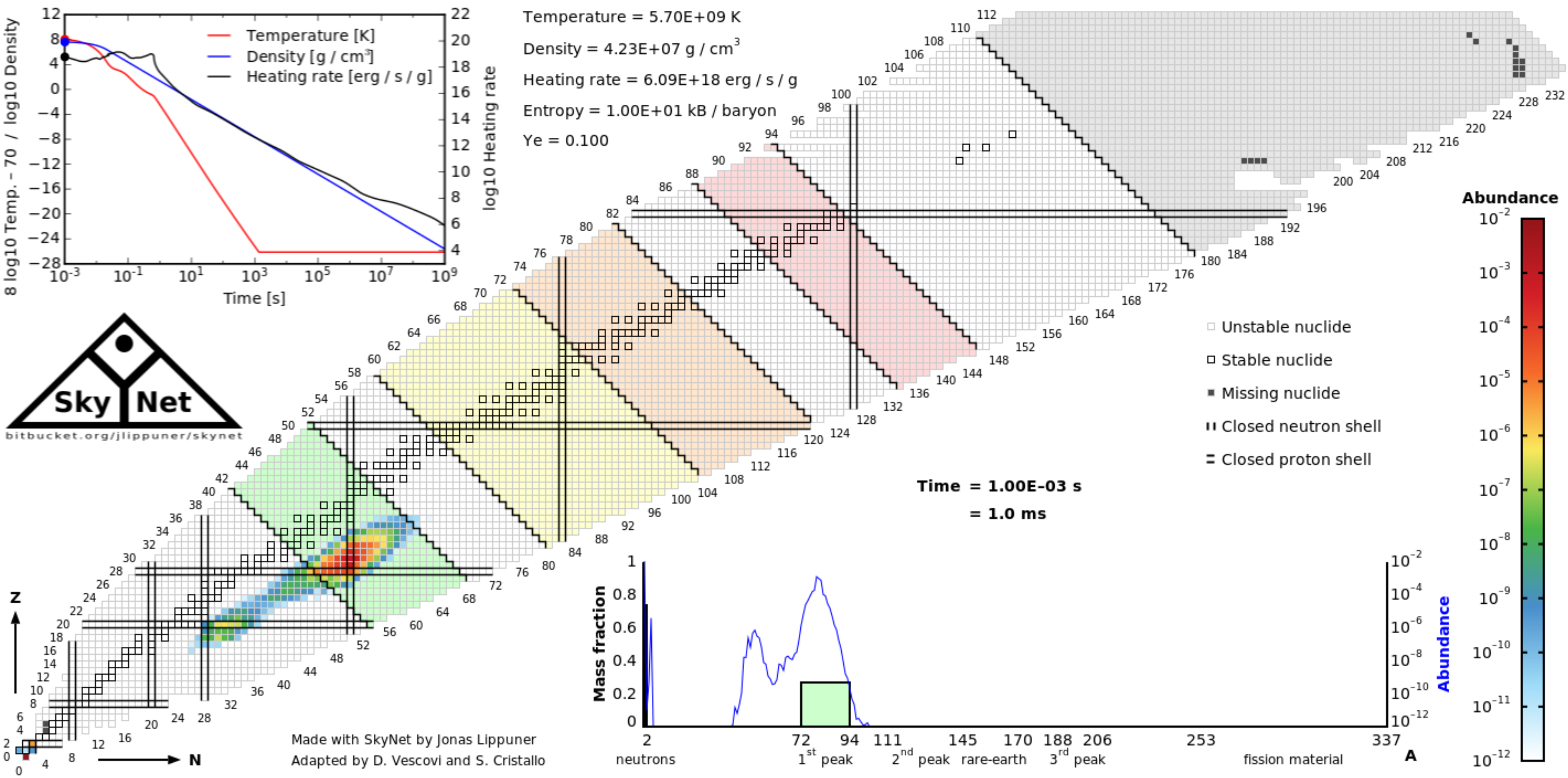

Role of fission for the robust r-process

- 1st peak is populated

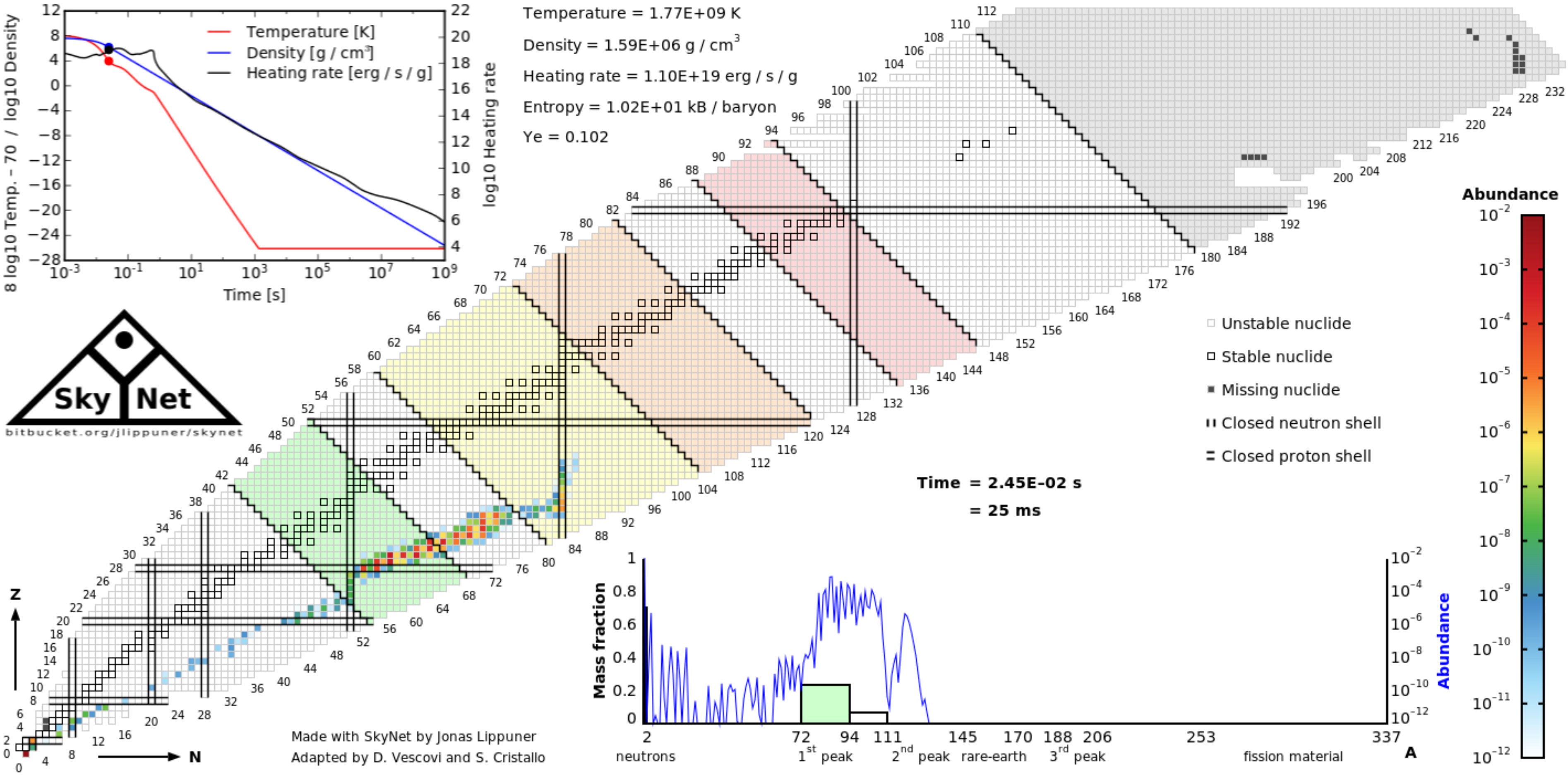

Role of fission for the robust r-process

- 2nd peak is populated

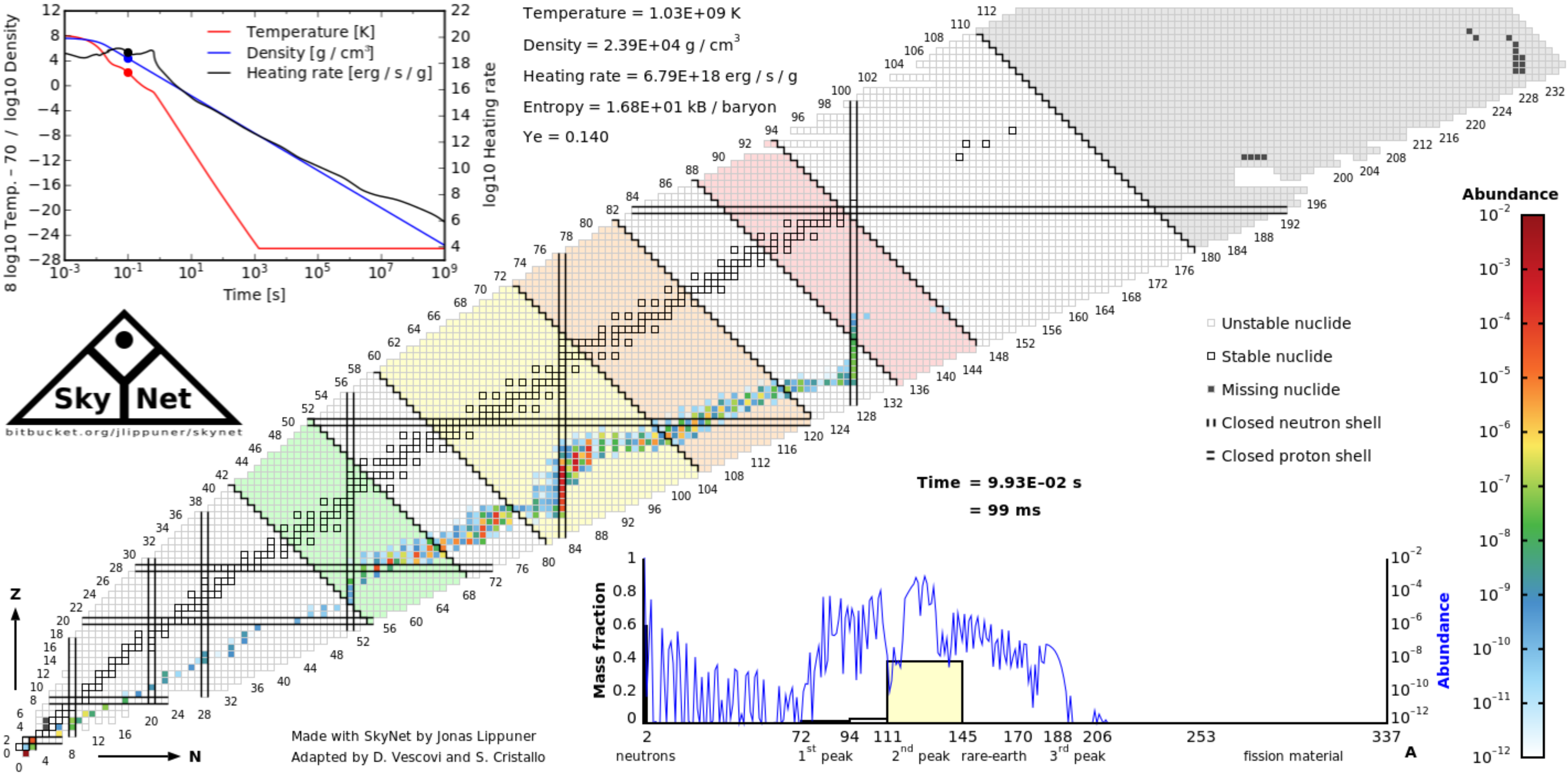

Role of fission for the robust r-process

- Fissile nuclei are produced

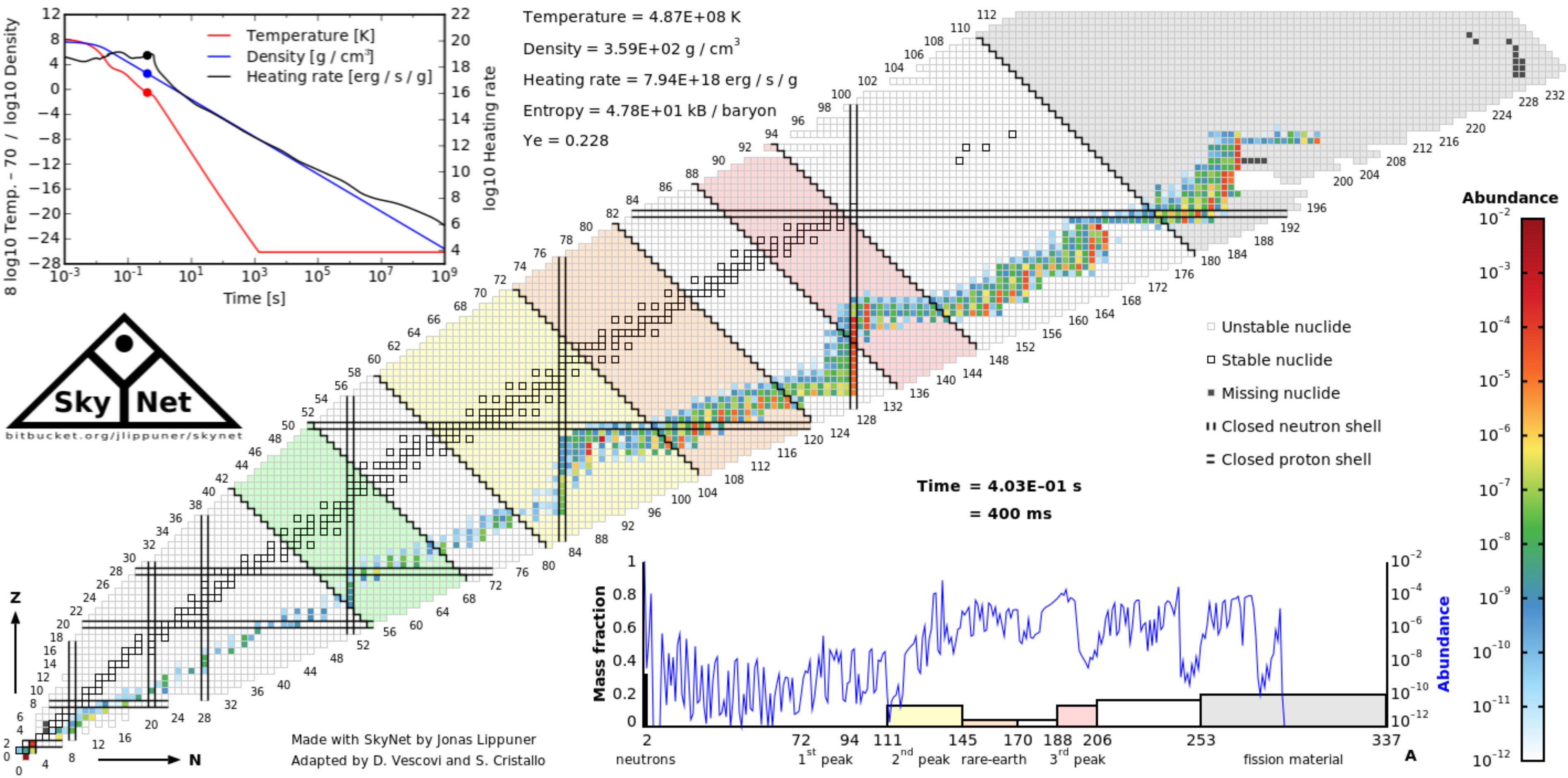

Role of fission for the robust r-process

- The fission of heavy nuclei leads to the creation of nuclei around the 2nd peak.
- Fission products continue to capture neutrons, leading to effective fission cycling

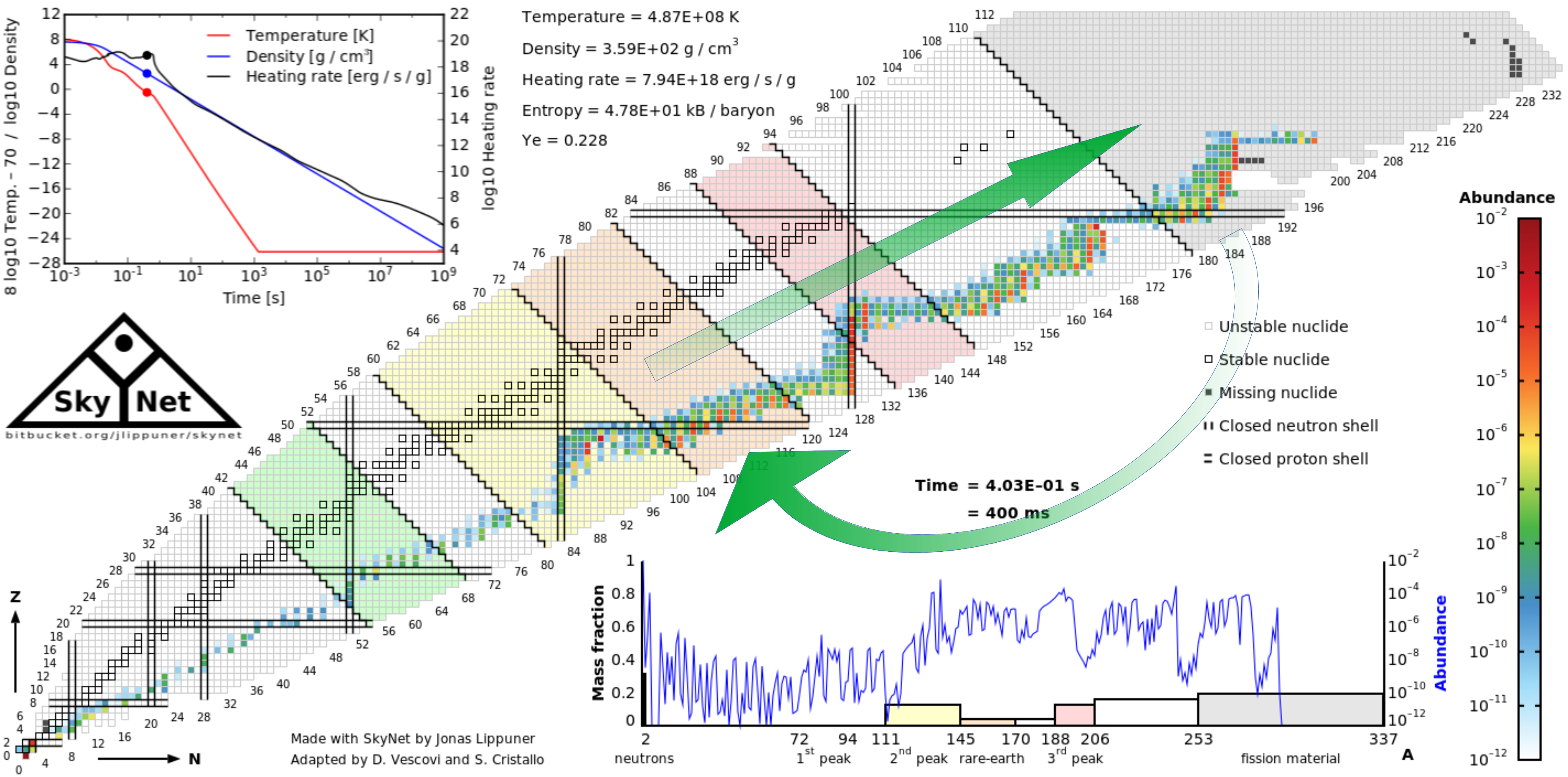

- An extremely neutron-rich environment guarantees the occurrence of several fission cycles before the *r*-process freezes out.

Nuclear physics quantities for modelling the r-process

1) Nuclear mass model
2) β-decay rates
3) Fission fragment distribution models

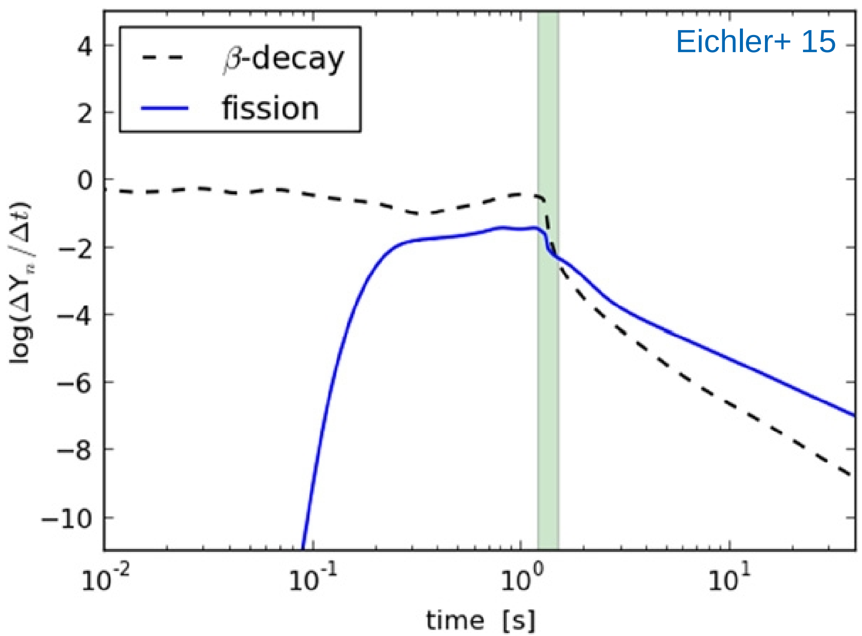

After the freeze-out the release of neutrons from fission dominates over β-delayed neutrons

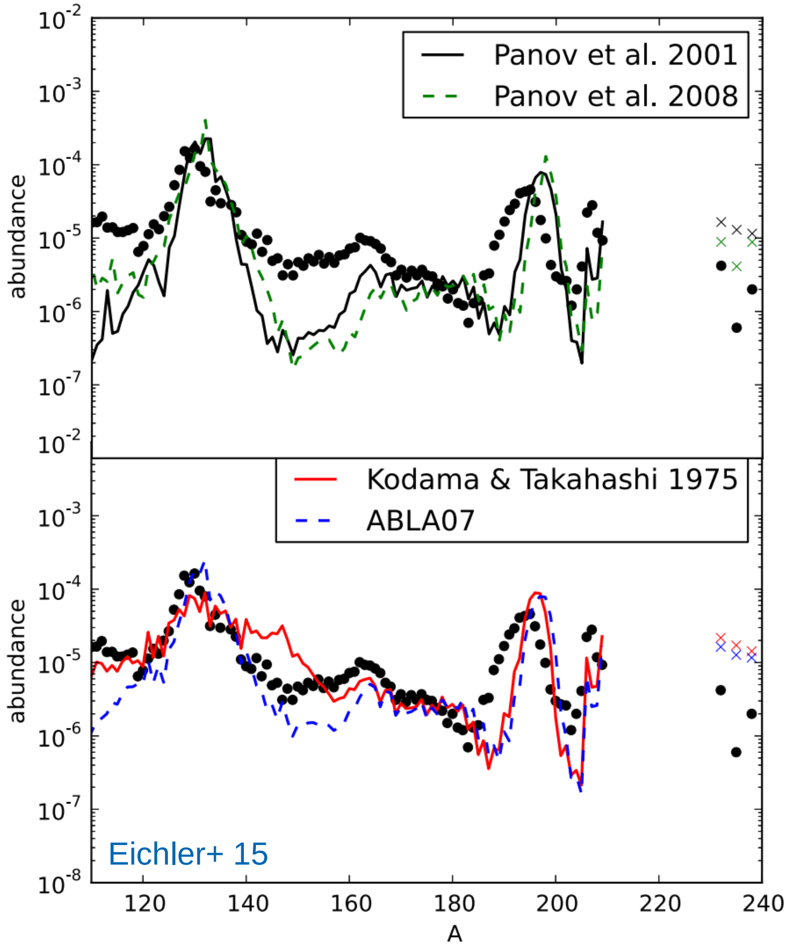

- <u>Late neutron captures</u> determine the position of the third *r*-process peak.
- <u>Fission fragments distribution</u> shapes the region around the second *r*-process peak.

Fission barriers and density levels above barrier

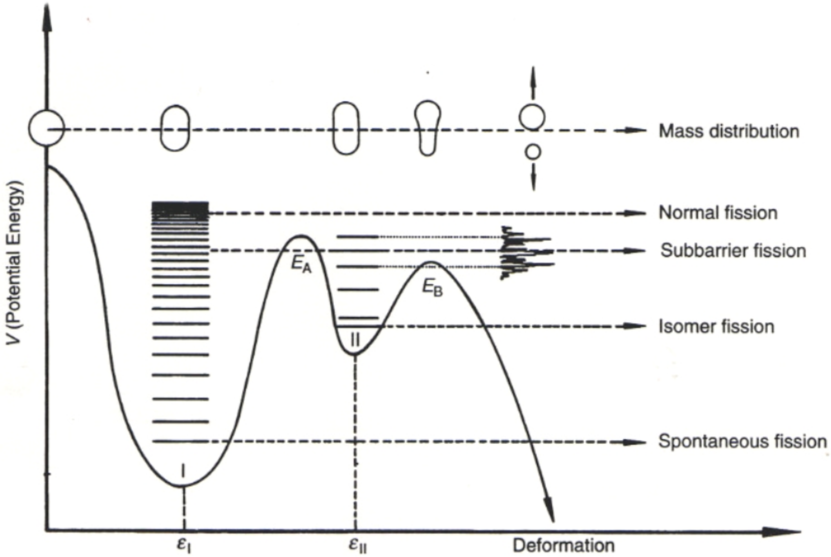

Independently of the channel, neutron-induced fission cross sections provide important data (fission barriers; level densities above barriers; etc.), which are needed to optimize (or validate) fission models for *r*-process nucleosynthesis.

Moreover, if the energy of the captured neutron is high enough to <u>re-emit neutrons</u> (1 or more) AND <u>activate the fission process</u>, multiple chance fission may occur. In this case, the study of multiple chance fission on more isotope of the same element <u>allows to refine fission models</u>.

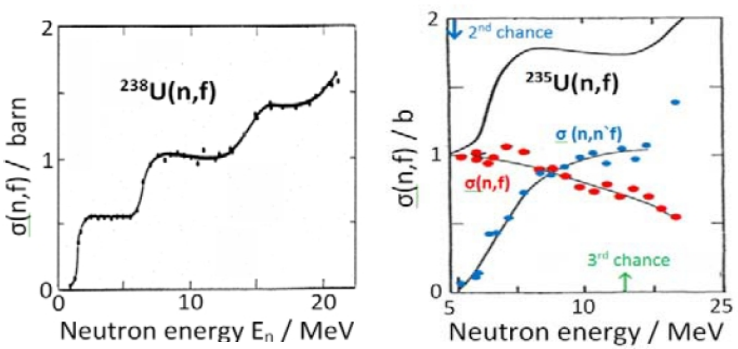

r-process nucleosynthesis

in low entropy environment ($s \sim$ a few tens of k_b /baryon)

→ Y_e dominant parameter

- $Y_e < 0.15$: robust *r*-process, due to several fission cycles
- $Y_e \lesssim 0.25$: 2nd and 3rd *r*-process peaks, but no first
- $Y_e \gtrsim 0.25$: up to 2nd *r*-process peak

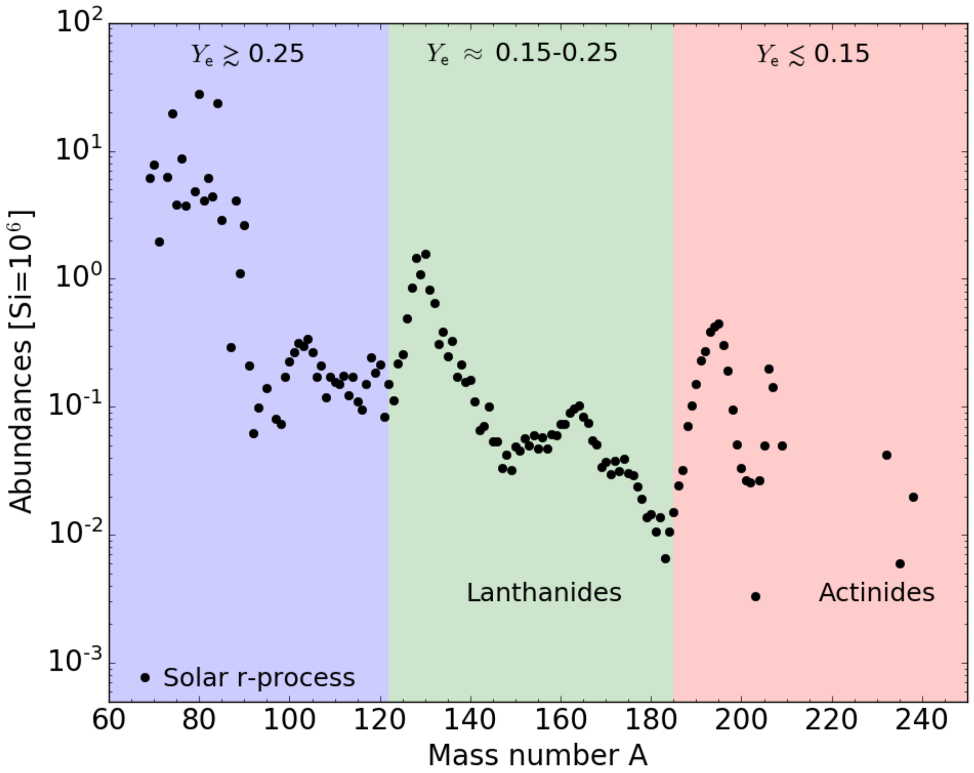

Production of lanthanides dramatically changes photon opacity (κ_γ), because of electrons filling *f*-shell in ionized states

- no lanthanides:
  low opacity ($\kappa_\gamma \lesssim 1$ cm²/g)

- presence of lanthanides: increased opacity ($\kappa_\gamma \gtrsim 10$ cm²/g)

Nuclear heating rate

- Radioactive decays of *r*-process elements release nuclear energy

$$\dot{Q}_{r-process} = \sum_{i \in reactions} Q_i \lambda_i$$

$$with \;\; Q = M_{initial} - M_{final}$$

$$\text{and} \;\; \lambda = decay\, rate$$

$Y_e \gtrsim 0.25$	$Y_e \lesssim 0.25$
weak *r*-process (A<130)	robust *r*-process (A>130)
"blue transients" peaking after ~ 1 day	"red transients" peaking after ~ 1 week

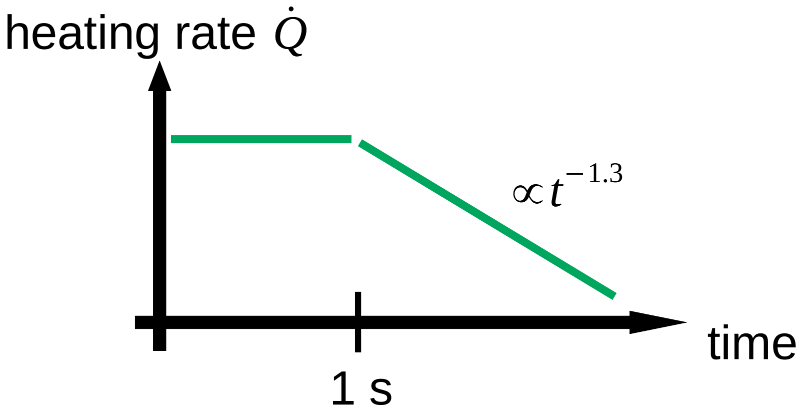

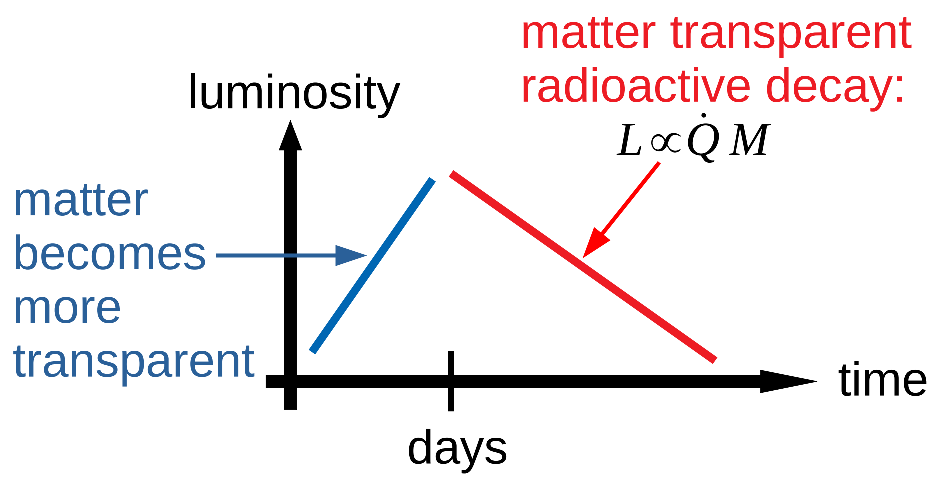

- key physics ingredients:
  1) ejecta mass, velocity, Y_e ➡ astrophysics
  2) opacity κ_γ ➡ atomic physics
  3) radioactive heating rate $\dot{Q}$ ➡ nuclear physics

Nuclear heating rate – Uncertanties I

How much variation can we expect from nuclear physics?

- Nucleosynthesis occurs near “neutron dripline”
- no experimental information
- rely on theoretical nuclear mass models

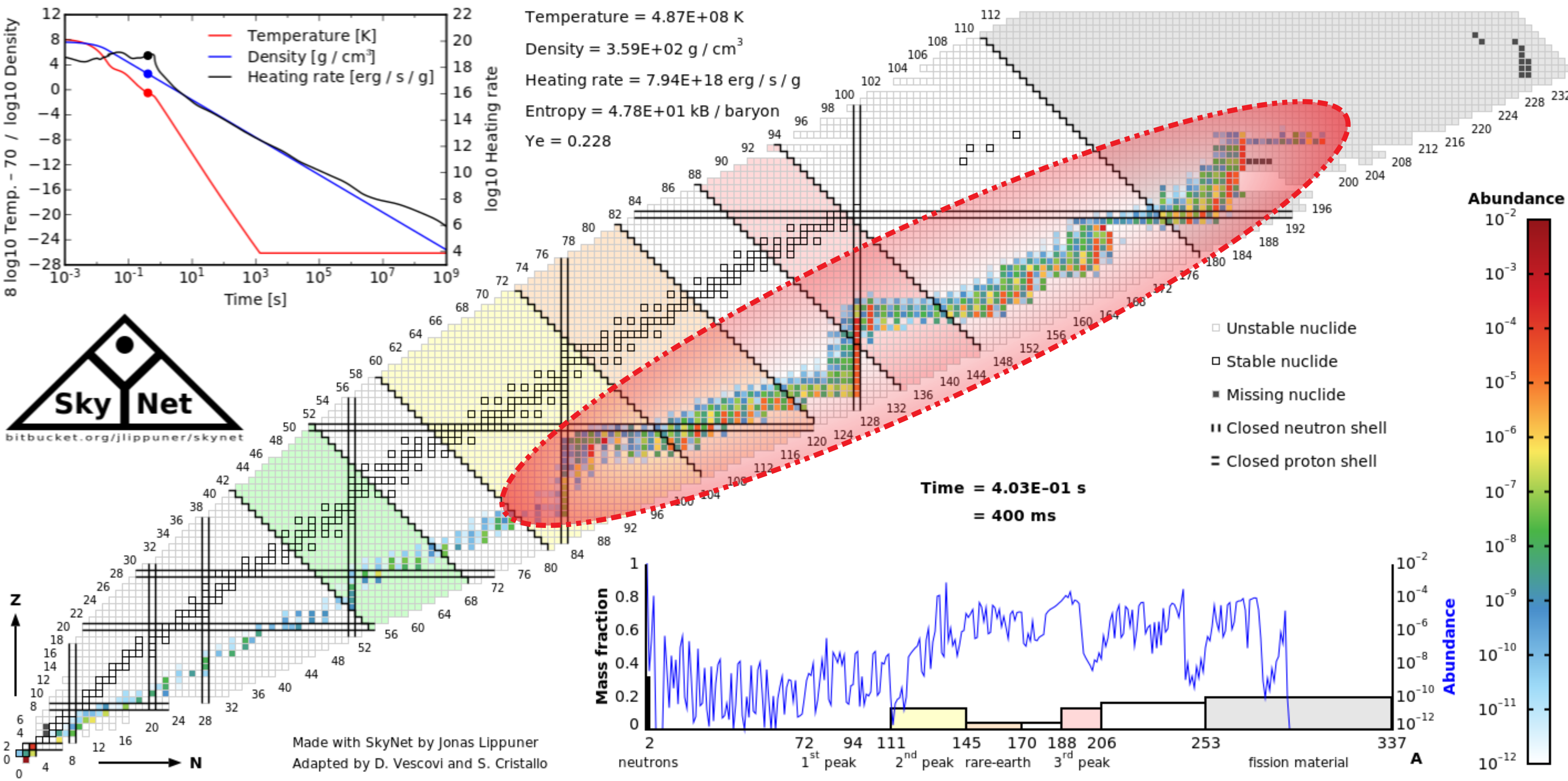

Nuclear heating rate – Uncertanties II

Comparing two frequently used nuclear mass models (Rosswog+ 2017):

1) "Finite Range Droplet Model" (FRDM; Möller+ 1995)
2) "Duflo Zuker Model" (DZ31; Duflo, Zuker 1995)

Abundances

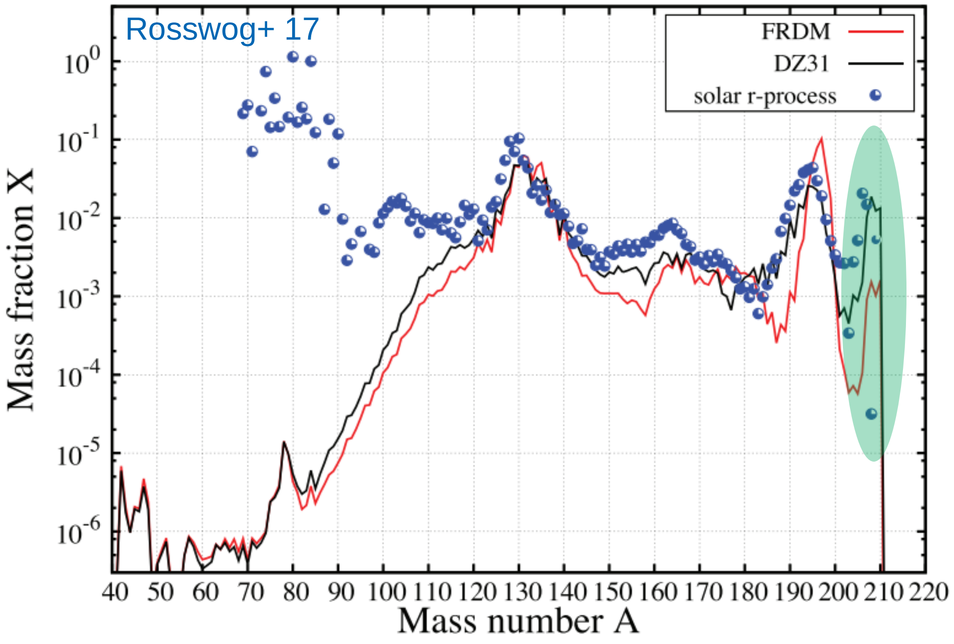

Heating rate

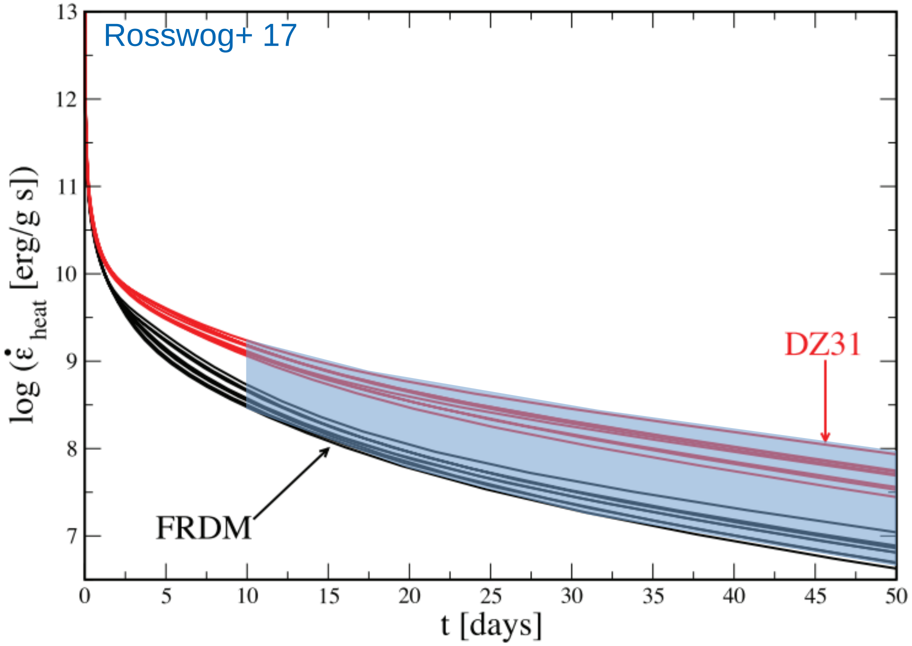

Trans-lead region is most relevant for heating (Barnes+ 2016):

- α-decays
- thermalization efficiency
- at relevant times difference of **factor ~5**

MCMC – Isotropic dynamical ejecta